Journal of Medicinal Chemistry

University of Sussex

Subscriber access provided by University of Sussex Library

Article

Small Molecules Simultaneously Inhibiting p53-Murine Double Minute 2 (MDM2) Interaction and Histone Deacetylases (HDACs): Discovery of Novel Multi-targeting Antitumor Agents

Shipeng He, Guoqiang Dong, Shanchao Wu, Kun Fang, Zhenyuan Miao, Wei Wang, and Chunquan Sheng

J. Med. Chem., **Just Accepted Manuscript** • DOI: 10.1021/acs.jmedchem.8b00664 • Publication Date (Web): 25 Jul 2018

Downloaded from http://pubs.acs.org on July 26, 2018

Just Accepted

"Just Accepted" manuscripts have been peer-reviewed and accepted for publication. They are posted online prior to technical editing, formatting for publication and author proofing. The American Chemical Society provides "Just Accepted" as a service to the research community to expedite the dissemination of scientific material as soon as possible after acceptance. "Just Accepted" manuscripts appear in full in PDF format accompanied by an HTML abstract. "Just Accepted" manuscripts have been fully peer reviewed, but should not be considered the official version of record. They are citable by the Digital Object Identifier (DOI®). "Just Accepted" is an optional service offered to authors. Therefore, the "Just Accepted" Web site may not include all articles that will be published in the journal. After a manuscript is technically edited and formatted, it will be removed from the "Just Accepted" Web site and published as an ASAP article. Note that technical editing may introduce minor changes to the manuscript text and/or graphics which could affect content, and all legal disclaimers and ethical guidelines that apply to the journal pertain. ACS cannot be held responsible for errors or consequences arising from the use of information contained in these "Just Accepted" manuscripts.

ACS Publications

is published by the American Chemical Society. 1155 Sixteenth Street N.W., Washington, DC 20036

Published by American Chemical Society. Copyright © American Chemical Society. However, no copyright claim is made to original U.S. Government works, or works produced by employees of any Commonwealth realm Crown government in the course of their duties.

Small Molecules Simultaneously Inhibiting p53-Murine Double Minute 2 (MDM2) Interaction and Histone Deacetylases (HDACs): Discovery of Novel Multi-targeting Antitumor Agents

Shipeng He[1,†], Guoqiang Dong[2,†], Shanchao Wu[2,†], Kun Fang[1], Zhenyuan Miao[2,*], Wei Wang[1,3,*], Chunquan Sheng[2,*]

[1] *School of Pharmacy, East China University of Science and Technology, Shanghai 200237, P. R. China*

[2] *Department of Medicinal Chemistry, School of Pharmacy, Second Military Medical University, 325 Guohe Road, Shanghai 200433, People's Republic of China*

[3] *Department of Chemistry and Chemical Biology, University of New Mexico, MSC03 2060, Albuquerque, NM 87131-0001, USA.*

ABSTRACT

p53-murine double minute 2 (MDM2) interaction and histone deacetylases (HDACs) are important targets in antitumor drug development. Inspired by the synergistic effects between MDM2 and HDACs, the first MDM2/HDACs dual inhibitors were identified, which showed excellent activities against both targets. In particular, compound **14d** was proven to be a potent and orally active MDM2/HDAC dual inhibitor, whose antitumor mechanisms were validated in cancer cells. Compound **14d** showed excellent *in vivo* antitumor potency in the A549 xenograft model, providing a promising lead compound for the development of novel antitumor agents. Also, this proof-of-concept study offers a novel and efficient strategy for multi-targeting antitumor drug discovery.

INTRODUCTION

p53 is a transcriptional factor that plays a key role in preventing tumor development.[1, 2] Approximately 50% of human cancers are related to the inactivation of p53.[3] Its interaction with human murine double minute 2 (MDM2) protein is the main inhibitory mechanism of the inactivation of transcriptional activity and tumor suppressor function of p53.[4-8] Blocking the p53-MDM2 protein-protein interaction with small-molecule inhibitors can re-activate the function of p53 and is emerging as a promising strategy in cancer therapy.[9] In the past few years, numerous small-molecule p53-MDM2 inhibitors were reported and several of them are currently being evaluated in preclinical or clinical trials.[10-14] However, clinical studies indicated that thrombocytopenia was the key adverse effect of MDM2 inhibitors, especially for daily administration.[15-17] Reducing the dose frequency is an effective strategy to avoid thrombocytopenia, and thus it is highly desirable to develop more efficient MDM2 inhibitors with prolonged dosing interval. Alternatively, simultaneous modulation of multiple targets by a single compound may generate superior efficacy and fewer side effects.[18, 19] For example, our group designed small-molecule inhibitors simultaneously targeting the MDM2 and NF-κB pathway, which achieved excellent *in vitro* and *in vivo* antitumor potency.[20, 21] Developing MDM2-based multi-targeting antitumor agents could serve as a promising strategy for novel antitumor drug development.

Histone deacetylases (HDACs), a class of epigenetic enzymes, play a crucial role in regulating the expression of tumor suppressor genes.[22, 23] In recent years, several

HDAC inhibitors, such as vorinostat (SAHA, **1**) and romidepsin, were approved by the FDA for the treatment of cancer.[24, 25] However, clinical application of the marketed HDAC inhibitors is generally restricted in the treatment of hematological malignancies, whose efficacy against solid tumors is poor.[26, 27] Moreover, most HDAC inhibitors are clinically used in combination with other antitumor agents to achieve synergistic effects.[28-31] Although drug combinations have the advantage of higher antitumor efficacy, they also suffered from enhanced adverse effects, unpredictable pharmacokinetic profiles, drug-drug interactions and so on.[32] In contrast, single-molecule with multi-targeting profiles are recently emerging as a promising alternative to combination therapy.[33] Our previous work and other studies have confirmed the effectiveness of HDAC-based multi-targeting antitumor agents, which showed improved antitumor activities and low toxicities.[34-36]

Recent studies indicated that HDAC inhibitors could synergistically enhance the antitumor effects of a variety of antitumor agents,[37] such as DNA damage reagents[38] and tubulin modulators[39]. In particular, HDAC inhibitors were capable of synergizing with MDM2 inhibitors in the suppression of tumor cells proliferation.[40] As shown in **Figure 1,** p53-MDM2 interaction acts by the auto-regulatory feedback loop mechanism in the physiological conditions. MDM2 is involved in inhibiting the function of p53 as a tumor suppressor by direct binding with p53 protein.[2, 41-43] Blocking p53-MDM2 interaction could release p53 from MDM2, thus restoring the tumor suppressor function of p53. On the other hand, functional inactivation of the tumor suppressor p53 is a fundamental step in tumorigenesis.[44] p53 acetylated at

Lys382 is one of the activated forms of p53 tumor suppressor and the acetylation of p53 is mediated by HDAC inhibitors.[45] Inhibition of HDACs or/and MDM2 may lead to the accumulation of activated p53. HDAC inhibitors could synergistically improve the antitumor activity of MDM2 inhibitors by modifying the hyperacetylation of p53.[40, 46] These evidence suggests that designing a single-molecule inhibitor simultaneously targeting HDAC and MDM2 could be an effective strategy in cancer therapy.[40]

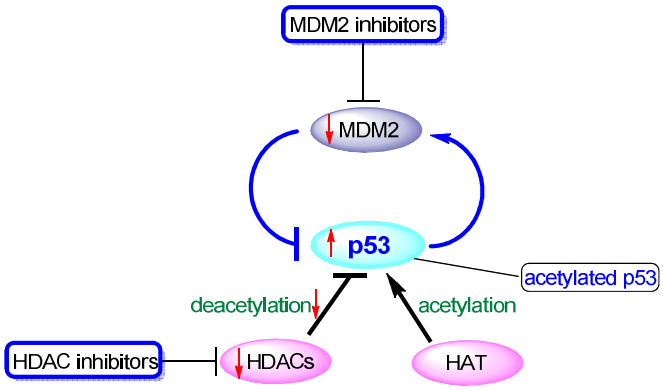

Figure 1. The relationship of MDM2 and HDACs in the signaling pathway.

Herein, the first MDM2/HDAC dual inhibitors were rationally designed, which showed excellent inhibitory activities against the both targets. Particularly, dual inhibitor **14d** showed excellent *in vivo* antitumor efficacy in the A549 xenograft model, highlighting the therapeutic value of this novel multi-targeting antitumor drug design strategy.

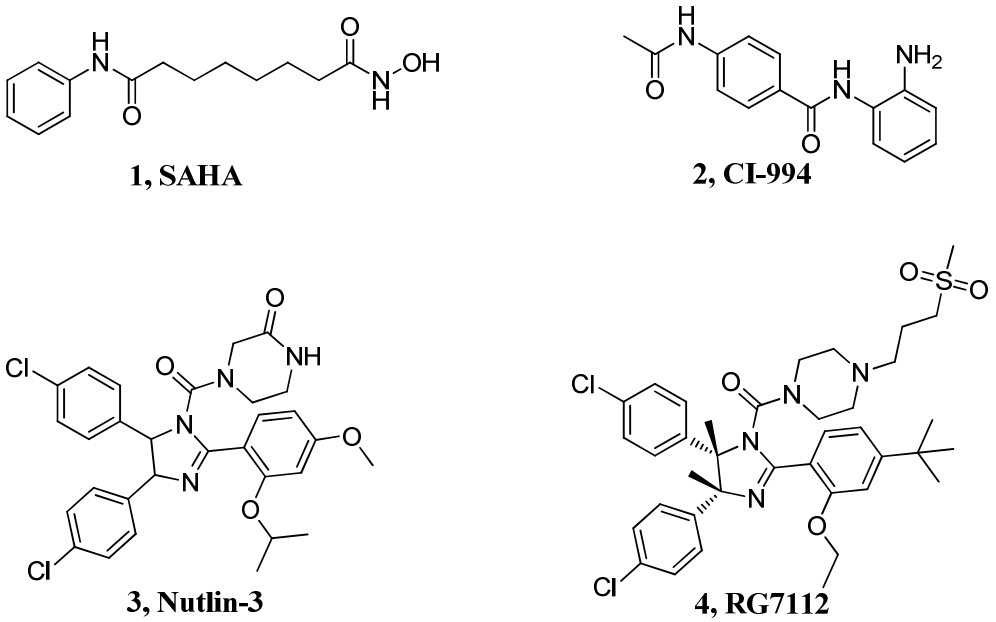

Figure 2. Chemical structures of HDAC and MDM2 inhibitors.

RESULTS AND DISCUSSION

Structure-based Design of Novel MDM2/HDAC Dual Inhibitors. Nutlins represent a classic class of MDM2 inhibitors (*e.g.*, compounds **3** and **4**, **Figure 2**).[47] Compound **3** showed good MDM2 inhibitory activity and has been widely used as a tool molecule or positive control to investigate the biological function of MDM2.[48] The optimization of Nutlins led to the discovery of compound **4** (RG7112) in the Phase 1 clinical trial.[49] The pharmacophore model of HDAC inhibitors can be divided into three parts: the cap group that interacts with the surface residues of HDAC, the linker and the zinc binding group (ZBG) that chelates with the active site Zn^{2+} ion (**Figure 3**).[50] Due to the presence of large hydrophobic domain at the HDACs surface, it is conceivable that appropriate substitution of the cap group of HDAC inhibitors by a chemical scaffold (or pharmacophore) from other type of anticancer agents could

generate new classes of multi-targeting molecules.[51]

According to the binding models of known HDACs and MDM2 inhibitors,[47, 50, 52, 53] compounds **1, 2** and nutlins were selected as the templets to design dual MDM2/HDAC inhibitors. The binding mode of compound **3** with MDM2 revealed that three functional groups on the imidazole scaffold mimicked Phe19, Trp23 and Leu26 residues in p53, which were projected into the binding pocket in MDM2 (**Figure 3**).[54] The N3 substitution of compound **3** was not buried inside the subpockets of MDM2 and directly exposed to the solvent, which was suitable to introduce a linker and the ZBG of HDAC inhibitors to obtain MDM2/HDAC dual inhibitors. Also, a polar side chain attached to the N3 position of compound **3** was favorable to adjust the physiochemical properties (*e.g.* aqueous solubility).[55]

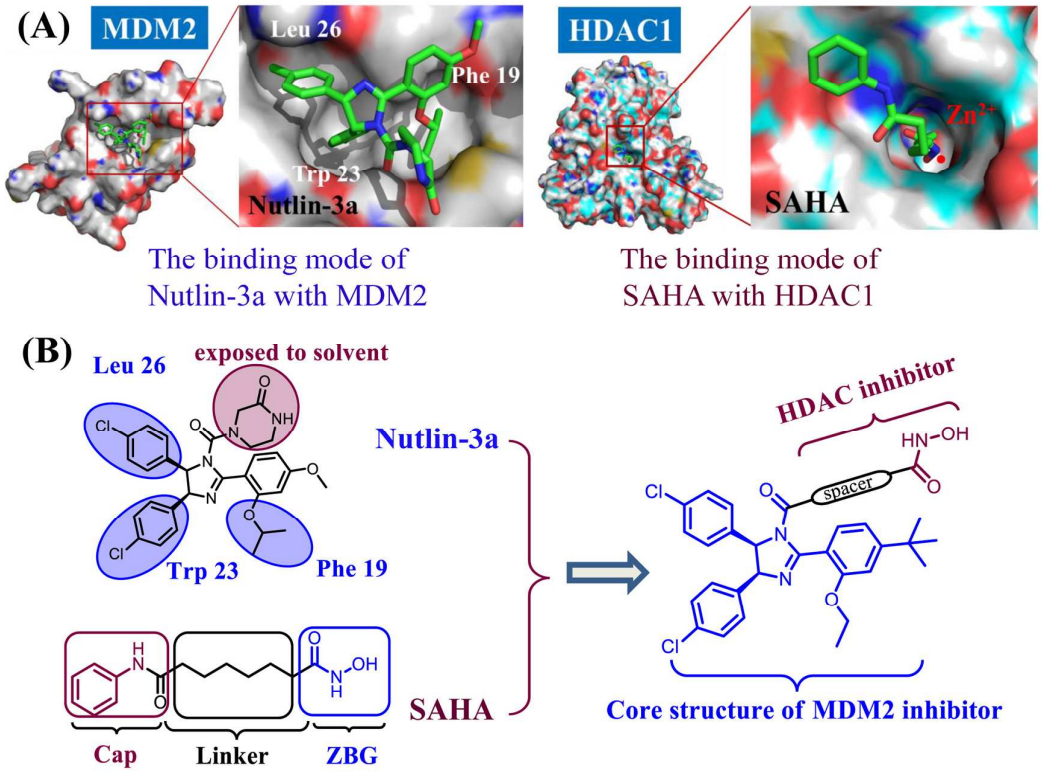

Figure 3. Design of MDM2-HDAC dual inhibitors. (A) The binding modes of

MDM2 and HDAC inhibitors; (B) Design rationale of MDM2-HDAC dual inhibitors.

Chemistry. As outlined in **Scheme 1**, treatment of intermediates **5** and **6** in the presence of $B(OH)_3$ and xylenes afforded imidazole **7**,[56] which was further reacted with triphosgene to obtain acyl chloride **8**.

Scheme 1[α]

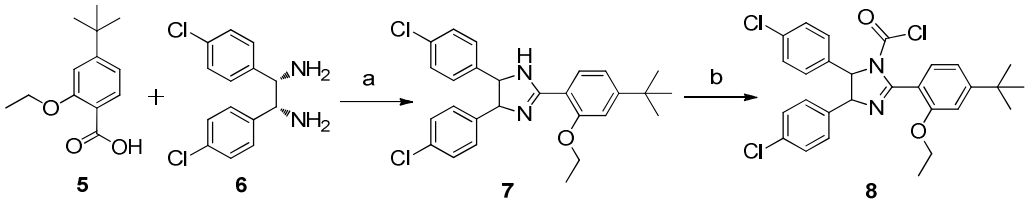

[α]Reagents and conditions: (a) $B(OH)_3$ (0.12 eq), xylenes, 145 °C, 6 h, yield 80%; (b) BTC (0.34 eq), rt, CH_2Cl_2, yield 82%.

Then, in the presence of DIPEA, intermediate **8** was condensed with commercially available aminoalkylesters **9a-d** to give amides **10a-d**, which was subsequently hydrolyzed to corresponding acids and condensed with *ortho*-phenylenediamine to afford target compounds **11a-d** (**Scheme 2**). Also, treatment of intermediates **10a-d** with freshly prepared hydroxylamine methanol solution yielded hydroximic acids **12a-d**. Similarly, target compound **13** was prepared from intermediate **8** via the condensation and ammonolysis reaction.

Scheme 2[α]

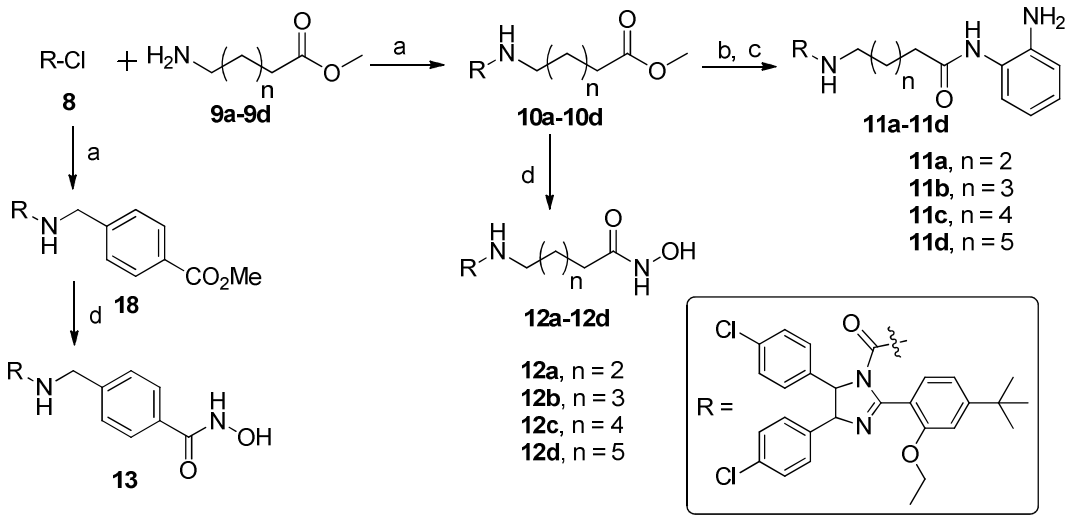

[α]Reagents and conditions: (a) DIPEA (1.2 eq), CH_2Cl_2, rt, 1.5 h, yield 70-90%; (b) LiOH (2.5 eq), THF: MeOH: H_2O = 3: 2: 1, rt, 2 h, yield 80-95%; (c) *Ortho*-Phenylenediamine (1.2 eq), HBTU (2.0 eq), TEA (2.0 eq), DMF, rt, 1-2 h, yield 55-70%; (d) NH_2OH (14 eq), MeOH, rt, 0.5 h, yield 88-95%.

A similar strategy was applied for the synthesis of piperazine-based conjugates **14a-e** (**Scheme 3**). Piperazines **19a-e** were reacted with **8** in the presence of Et_3N and CH_2Cl_2 to give esters **20a-e** in good yield. Then, the synthesis of target compounds **14a-e** was similar to that of compounds **12a-d**. Compounds **15a** and **15b** were synthesized via the condensation and ammonolysis reaction from intermediate **8**. Starting from piperidine intermediates **22a-b** and **23**, target compounds **16a-b** (**Scheme 4**) were obtained by a similar protocol described in **Scheme 1**.

Scheme 3[α]

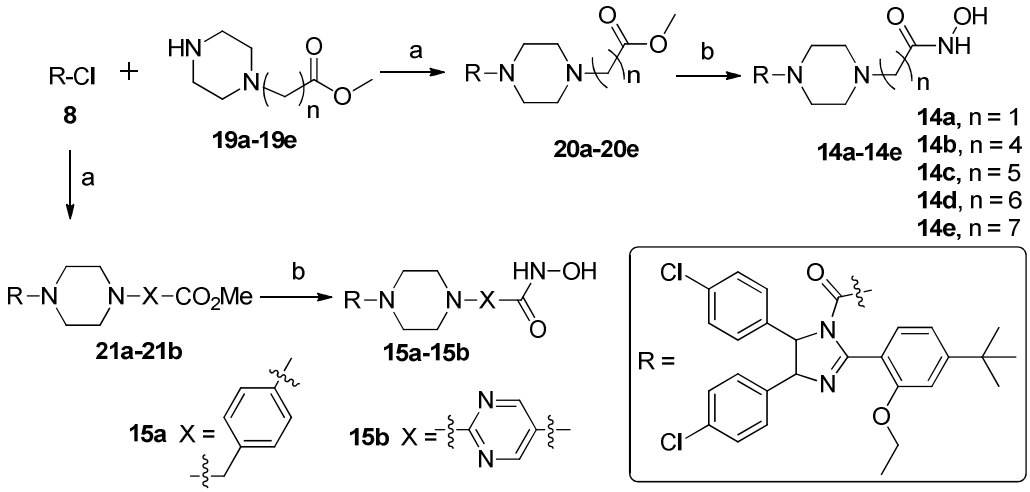

[α]Reagents and conditions: (a) Et_3N (1.2 eq), CH_2Cl_2, rt, 1 h, yield 70-92%; (b) NH_2OH (14 eq), MeOH, rt, 45 min, yield 88-92%.

Scheme 4[α]

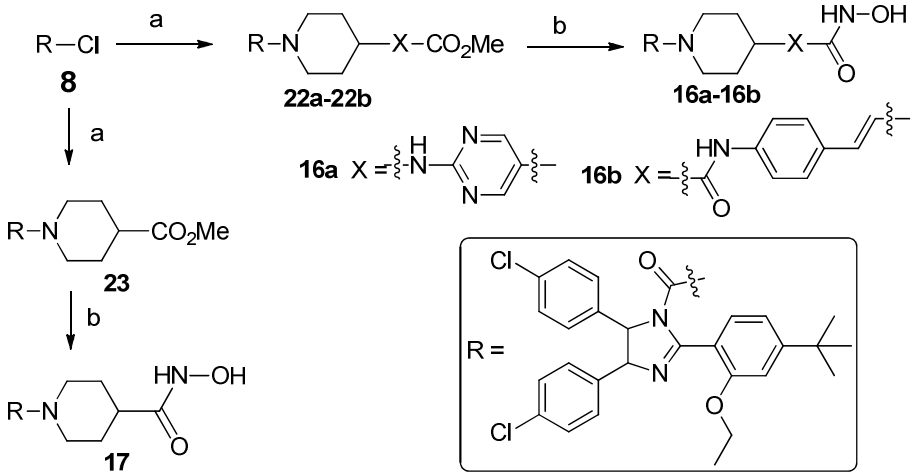

[α]Reagents and conditions: (a) DIPEA (1.2 eq), CH_2Cl_2, rt, 1 h, yield 90-95%; (b) NH_2OH (14 eq), MeOH, rt, 1 h, yield 85-95%.

Biochemical Evaluations and Structure-activity Relationships. MDM2 and HDACs inhibitory activities were evaluated by the fluorescence polarization binding assay[21] and fluorescent activity assay[34], respectively, using compounds **1-3** as the positive controls. Initially, *ortho*-aminoanilide was used as the ZBG (**11a-d**). These compounds generally showed good inhibitory activity against MDM2 (K_i range: 0.96~1.43 μM). However, compounds **11a** and **11b** were inactive against HDAC1. The extension of the linker length led to improved activity against HDAC1 (*e.g.* compound **11d**, IC_{50} = 3.59 μM). Interestingly, the replacement of the *ortho*-aminoanilide by hydroxamate acid (**12a-d**) resulted in enhanced activities against both MDM2 and HDAC1 (**Table 1**). The linker length had little impact on the MDM2 inhibitory activity and compounds **12a-d** had a K_i value ranging from 0.28 μM to 0.34 μM. In contrast, with the increase of the linker length, the HDAC1 inhibitory activity was improved accordingly, indicating that a long alkyl linker might be beneficial to HDAC1 binding. Among them, compound **12d** showed balanced activity towards both MDM2 (K_i = 0.34 μM) and HDAC1 (IC_{50} = 0.27 μM). Moreover, the flexible alkyl linker was replaced by a rigid aromatic-based chain (compound **13**). Unfortunately, its MDM2/HDAC1 inhibitory activity was decreased.

Table 1. MDM2 Binding Affinity and HDAC Inhibitory Activities of the Target Compounds

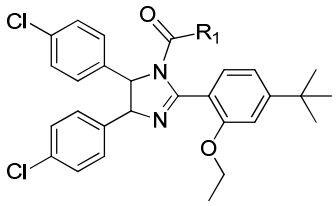

Compound	R_1	MDM2	HDAC1
		K_i (μM) [a]	IC_{50} (μM) [a]
11a	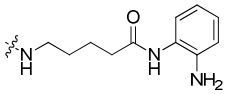	0.96 ± 0.032	＞20
11b	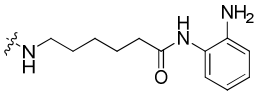	1.43 ± 0.311	＞20
11c	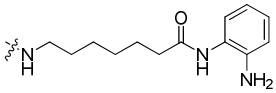	0.62 ± 0.107	6.07 ± 0.88
11d	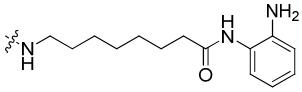	1.02 ± 0.223	3.59 ± 0.67
12a	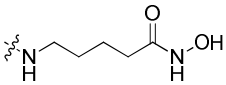	0.33 ± 0.029	2.92 ± 0.72
12b	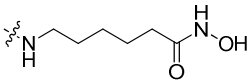	0.28 ± 0.034	1.13 ± 0.56
12c	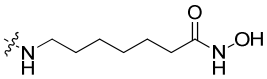	0.32 ± 0.026	0.89 ± 0.09
12d	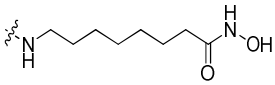	0.34 ± 0.041	0.27 ± 0.04
13	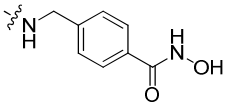	0.58 ± 0.042	3.70 ± 0.06
1		>20	0.056 ± 0.015
2		NT[b]	1.09 ± 0.31

3	0.14 ± 0.04	NT[b]

[a] Values represent a mean ± SD of at least two independent experiments. [b]NT = Not tested.

Next, piperazine or piperidine was incorporated into the linker to improve the binding affinities toward both targets as well as the water solubility (**Table S1** in **Supporting Information**). Generally, piperazine derivatives **14a-e** showed better MDM2 inhibitory activities than compounds **12a-d** (**Table 2**). In particular, compound **14a** had excellent MDM2 binding affinity (K_i = 0.07 μM). Meanwhile, HDAC1 inhibitory activities of compounds **14a-e** were improved accordingly. Similar to compounds **12a-d**, a long alkyl linker was helpful to enhance HDAC1 inhibitory activities. Among them, compounds **14b-e** generally showed balanced inhibition towards MDM2/HDAC1. When aromatic groups were introduced into the linker, decreased HDAC1 binding activity was observed for phenyl derivative **15a**. Pyrimidine derivative **15b** showed improved activity against HDAC1, whereas its MDM2 binding affinity was obviously decreased. For the piperidine derivatives (**16a-b, 17)**, compound **17** showed the best MDM2 binding affinity (K_i = 0.06 μM) among all the synthesized compounds, whereas its HDAC1 inhibitory activity was poor. Further incorporation of the aromatic groups into the linker (compound **16b**) was beneficial for the HDAC1 inhibitory activity, but the activities for MDM2 were significantly decreased.

Table 2. MDM2 Binding Affinity and HDAC Inhibitory Activities of Target Compounds

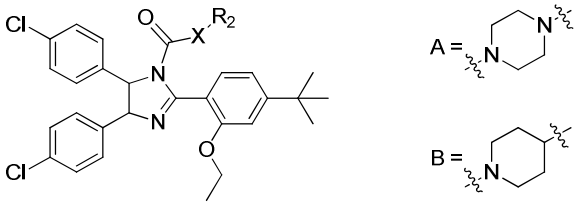

Compound	X	R_2	MDM2	HDAC1
			K_i (μM) [α]	IC_{50} (μM) [α]
14a	A	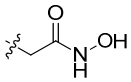	0.07 ± 0.01	4.20 ± 0.59
14b	A	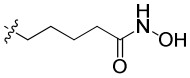	0.17 ± 0.02	0.98 ± 0.08
14c	A	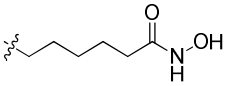	0.17 ± 0.03	0.97 ± 0.13
14d	A	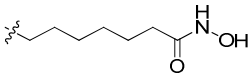	0.11 ± 0.03	0.82 ± 0.04
14e	A	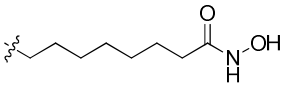	0.29 ± 0.04	0.41 ± 0.05
15a	A	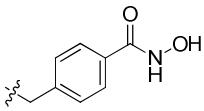	0.26 ± 0.03	3.51 ± 0.71
15b	A	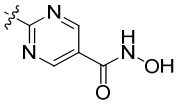	1.05 ± 0.43	0.31 ± 0.07
16a	B	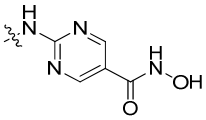	0.46 ± 0.034	1.01 ± 0.71
16b	B	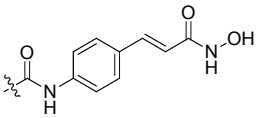	2.65 ± 0.79	0.97 ± 0.07
17	B	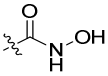	0.057 ± 0.028	9.72 ± 1.11
1			>20	0.056 ± 0.015

2	NT[b]	1.09 ± 0.31
3	0.14 ± 0.04	NT[b]

[a]Values represent a mean ± SD of at least two independent experiements. [b]NT = Not tested.

***In vitro* Antiproliferative Assay.** Given the potent enzyme inhibitory activities, the antiproliferative activities of the MDM2/HDAC dual inhibitors were investigated against p53-wild A549 (human lung cancer), HCT-116 (human colon cancer) and MCF-7 (human breast cancer) cell lines by the CCK8 assay. As shown in **Table 3**, most compounds showed good growth inhibition activities against the three human cancer cells. Moreover, they were more effective against the A549 and HCT116 cells than MCF-7 cells. The *in vitro* antitumor activities were generally consistent with the inhibitory activities towards the two targets. For example, compounds **14a-e** with better MDM2/HDAC1 inhibitory activity were also more potent than compounds **12a-d**. Among them, compound **14d** exhibited the best antiproliferative activity, particularly for A549 cell line (IC_{50} = 0.91 μM), which was more potent than the three positive drugs. On the other hand, the improvement of solubility by introducing polar group may be one of the reasons for the increasing the cellular activity.[57] For example, compound **14d** had better solubility than **12c** after introducing the piperazine group (**Table S1** in **Supporting Information**), and thus the antiproliferative activity of compound **14d** was superior to that of compound **12c**. In addition, the inhibitory activities against the p53-deleted NCI-H1299 cells (human

non-small cell lung cancer) were tested. The results revealed most compounds had relatively poor inhibitory activities towards NCI-H1299 cells compared with those of p53-wild A549 cells (**Table 3**). For example, compound **14d** showed an IC_{50} value of 4.16 μM and 0.91μM against NCI-H1299 and A549 cells, respectively. Considering the molecular and cellular activities, compound **14d** was subjected to further evaluations.

Table 3. Antiproliferative Activity of Target Compounds against Four Solid Tumor Cell Lines (IC_{50}, μM)[a]

Compound	A549	HCT116	MCF-7	NCI-H1299
11a	18.35 ± 0.63	13.86 ± 0.68	29.14 ± 1.82	15.63 ± 2.70
11b	20.27 ± 1.71	21.80 ± 1.11	>100	19.10 ± 1.68
11c	15.97 ± 0.77	10.13 ± 2.03	>100	17.51 ± 2.92
11d	15.16 ± 0.83	9.91 ± 1.07	20.26 ± 3.27	19.58 ± 2.20
12a	9.34 ± 1.27	10.70 ± 0.98	12.77 ± 1.31	16.22 ± 1.36
12b	5.72 ± 0.76	7.15 ± 1.03	10.55 ± 1.25	10.38 ± 0.68
12c	5.97 ± 0.25	7.09 ± 0.64	7.23 ± 0.92	7.65 ± 0.83
12d	4.85 ± 0.89	5.03 ± 0.75	7.92 ± 1.48	9.06 ± 1.09
13	7.64 ± 1.18	9.10 ± 0.81	13.31 ± 2.73	7.71 ± 0.57
14a	4.32 ± 0.66	5.88 ± 0.84	11.67 ± 1.30	11.54 ± 2.36
14b	3.78 ± 0.82	5.21 ± 0.69	9.80 ± 0.76	12.93 ± 2.07
14c	2.91 ± 0.32	4.03 ± 1.02	7.26 ± 1.13	9.39 ± 0.72
14d	0.91 ± 0.09	1.08 ± 0.46	4.34 ± 0.83	4.16 ± 1.13

14e	2.01 ± 0.82	1.71 ± 0.79	4.83 ± 0.97	7.76 ± 1.09
15a	2.17 ± 0.98	2.03 ± 0.92	3.97 ± 0.87	3.00 ± 0.38
15b	1.97 ± 0.79	0.98 ± 0.07	3.46 ± 0.95	5.45 ± 0.82
16a	3.11 ± 0.48	3.24 ± 0.75	2.68 ± 0.47	7.91 ± 1.06
16b	7.59 ± 1.05	9.64 ± 1.21	7.22 ± 0.99	9.36 ± 0.59
17	2.99 ± 0.51	9.30 ± 0.66	10.07 ± 1.02	9.87 ± 1.08
1	2.01 ± 0.99	1.18 ± 0.42	4.83 ± 0.69	4.92 ± 0.63
2	10.17 ± 1.22	9.83 ± 1.96	13.16 ± 3.14	6.79 ± 1.01
3	11.65 ± 1.09	9.07 ± 0.92	8.50 ± 0.93	19.76 ± 2.11

[a]IC_{50} values are the mean of at least three independent assays, presented as mean ± SD.

HDACs Isoform Selectivity of Compound 14d. In order to test the HDAC isoform selectivity profile, compound **14d** was selected to assay the enzyme inhibitory activities against HDAC1-3, HDAC6 and HDAC8 (**Table 4**). The results revealed that compound **14d** exhibited remarkable selectivity for HDAC6 (IC_{50} = 17.5 nM) over other isoforms. In contrast, it inhibited HDAC1 (IC_{50} = 820 nM), HDAC2 (IC_{50} = 420 nM) and HDAC3 only in the sub-micromolar range. Similar to positive compound **1**, compound **14d** was less active activity against HDAC8 (IC_{50} = 1224 nM).

Table 4. HDACs Isoform Selectivity of Compounds 1 and 14d (IC_{50}, nM)[α]

	1	**14d**
HDAC1	45.0 ± 3.1	821 ± 12

HDAC2	153.1 ± 41.0	420.5 ± 13.0
HDAC3	29.0 ± 3.1	178.3 ± 6.2
HDAC6	16.3 ± 1.6	17.5 ± 1.3
HDAC8	3970 ± 379	1224 ± 172

[a]IC_{50} values are the mean of at least three independent assays, presented as mean ± SD.

Effects of Compound 14d on p53 and MDM2 Expression. Next, we investigated the effects of compound **14d** on the levels of p53 and MDM2 expression in A549 cells by Western blotting analysis using compound **3** as the positive control (**Figure 4**). Treatment with compound **14d** or **3** in A549 cells both dose-dependently increased the protein level of p53, as well as MDM2 at the 24 h time point. The results indicated that compound **14d** had similar effects to compound **3** in inducing the p53 and MDM2 expression within A549 cells.

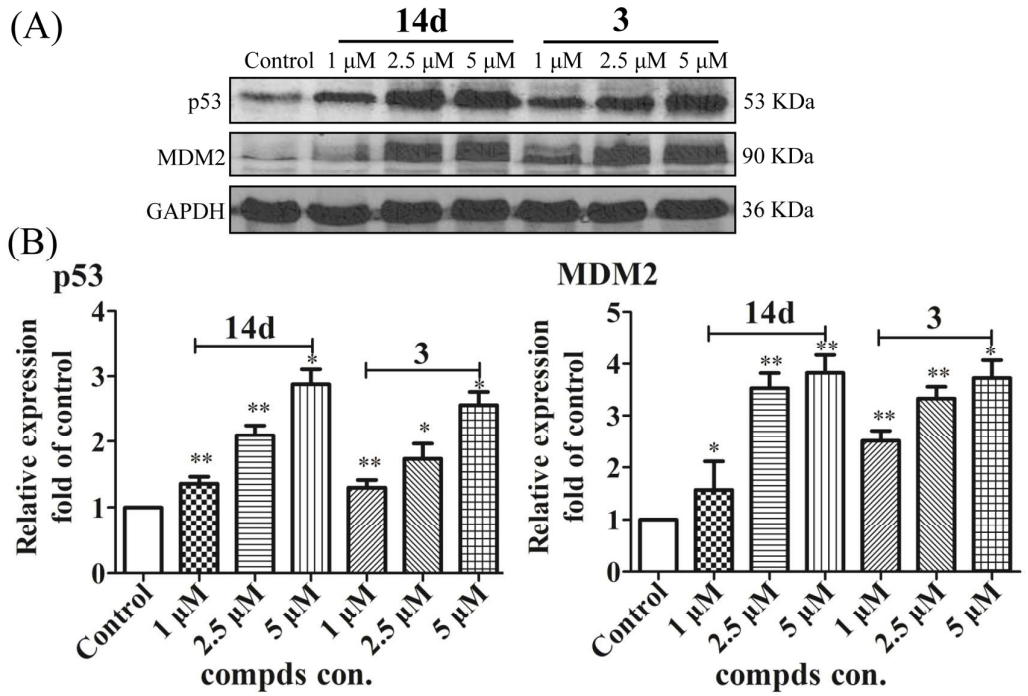

Figure 4. Western blotting analysis of p53 and MDM2 expression by compound **14d**. (A) Effects of compounds **14d** and **3** on the level of p53 and MDM2 in human lung cancer A549 cells using Western blotting analysis after the treatment for 24 h. GAPDH was used as a loading control. (B) Quantitative analysis of Western blotting using ImageQuant (Molecular Dynamics, U.S.). Protein p53 and MDM2 were analyzed in A549 cells, respectively. Data were presented as means ± SEM, n = 3. * $P < 0.05$ and ** $P < 0.01$ *vs* control group.

Effects of Compound 14d on Histone and *α*-Tubulin Acetylation. In order to probe the contribution of HDACs inhibition to the cytotoxic activity of compound **14d**, the intracellular acetylation level of histone 3 and histone 4 (**Figure 5**), two common substrates for HDAC (1, 2 and 3), were determined in A549 cells by the Western blotting. Similar to HDAC inhibitor **1**, compound **14d** dose-dependently increased the acetylation level of histone 3 and of histone 4 in A549 cells. Compound **14d** was further subjected for evaluation of intracellular HDAC6 inhibition. The effects of compound **14d** on the acetylation level of α-tubulin, a known substrate for HDAC6, are shown in **Figure 5**. Exposure to compound **14d** for 24 h led to the increase of α-tubulin acetylation in A549 cells. These results demonstrated that the inhibition of intracellular HDAC1 and HDAC6 was one of the mechanisms of bioactivity of compound **14d**.

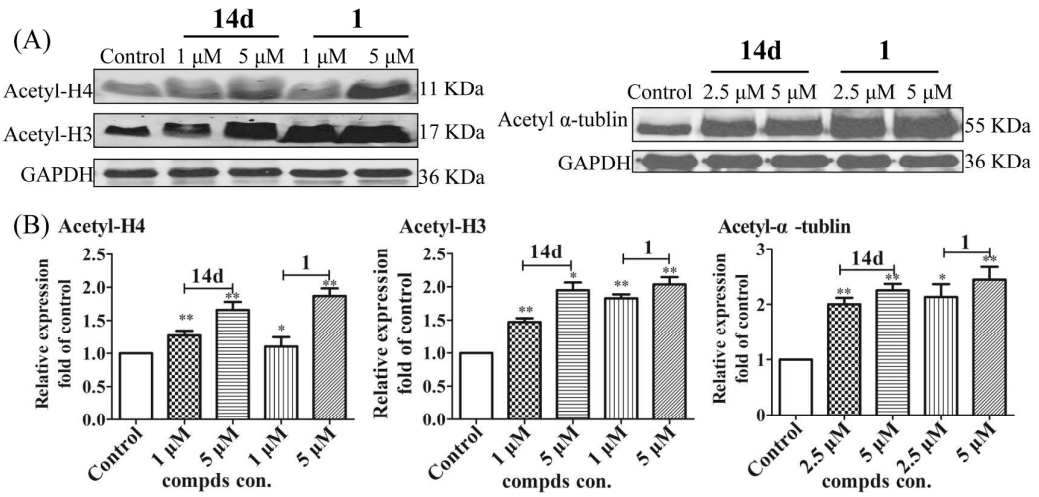

Figure 5. Western blotting analysis of histone and *α*-tubulin acetylation by compound **14d**. (A) Effects of compounds **14d** and **1** on the levels of histone 3 and histone 4 acetylation, α-tubulin acetylation in lung cancer A549 cells using Western blotting analysis after the treatment for 24 h. (B) Quantitative analysis of Western blotting with ImageQuant (Molecular Dynamics, U.S.). Histone 3 and 4 acetylation and *α*-tubulin acetylation were analyzed in A549 cells, respectively. Data were presented as means ± SEM, n = 3. * $P < 0.05$ and ** $P < 0.01$ *vs* control group.

Flow Cytometry Analysis. It was reported that p53-MDM2 inhibitor **3** arrested wild-type p53 cancer cell lines at the G0/G1 phase and depleted the S-phase compartment.[47] HDAC inhibitor **1** induced cell cycle arrest at the G0/G1 phase through transcriptional activation of genes such as cell cycle-regulated genes in a p53-independent manner.[37] Compound **1** could also arrest the G2/M phase in some human cancer cell lines.[58, 59] To investigate the cellular mechanisms of compound **14d**, its effects on the cell cycle progression were tested in A549 cells by the flow cytometry analysis (**Figure 6**). As compared to the vehicle, treatment with 1 μM of

compounds **14d**, **1**, and **3**, respectively, led to the increase of G0/G1 fraction. Compounds **14d** and **3** were also able to arrest A549 cell-cycle progression in the G0/G1 segment at higher concentration (5 μM). Meanwhile, compound **1** also resulted in the increase of the G2/M fraction at the same concentration. The results indicated that compound **14d** could significantly arrest the A549 cell cycle at the G0/G1 phase.

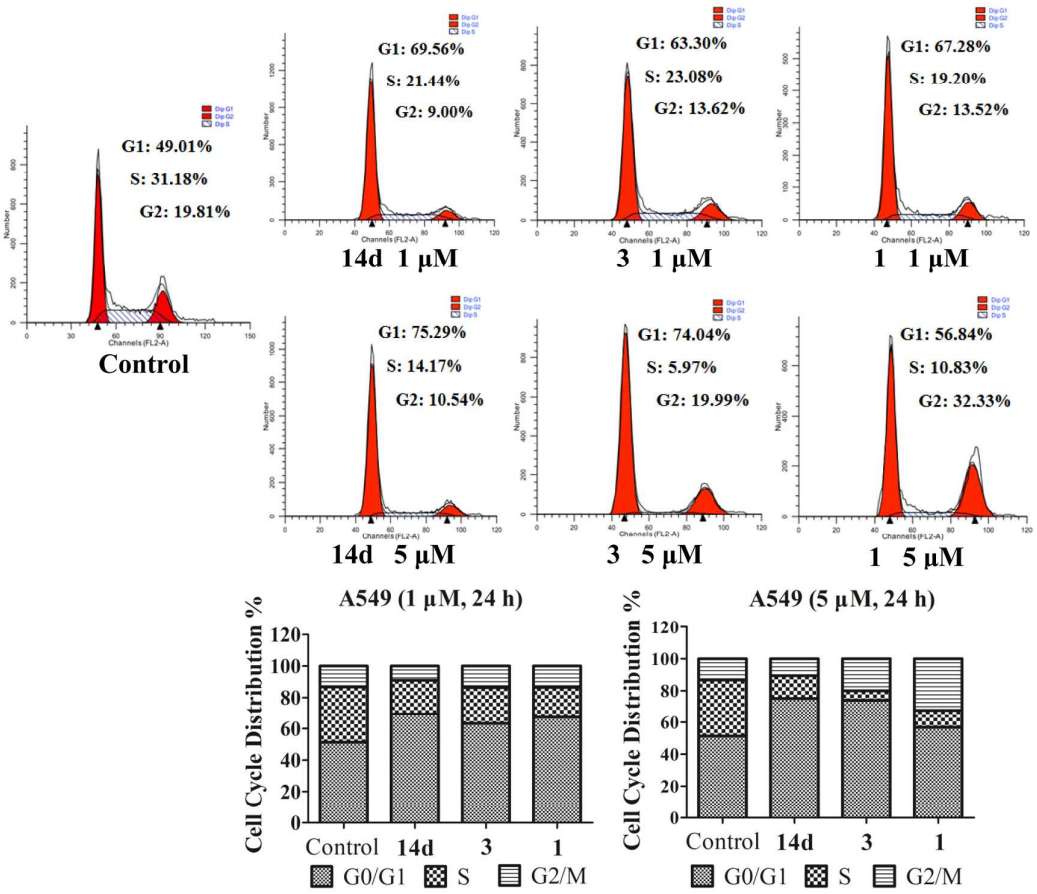

Figure 6. Cell cycle analysis of compound **14d** by flow cytometry. Human non-small lung cancer cells (A549) were treated with increasing concentrations of compound **14d** or reference compounds for 24 h. The data are representative of two independent experiments.

Previous studies revealed that inactivation of HDAC and/or MDM2 could increase the percentage of apoptosis cells.[47, 60, 61] Flow cytometry analysis was performed to determine the cell apoptosis effects of compound **14d** towards A549 cells. As shown in **Figure 7**, compound **14d**, as well as **1** and **3**, could significantly induce apoptosis in a dose-dependent manner. At the concentration of 5 μM, compound **14d** induced 33.57% of cell apoptosis, which was higher than that of compounds **1** (31.99%) and **3** (15.32%), indicating that inactivation of HDAC and/or MDM2 could increase the percentage of apoptosis cells.

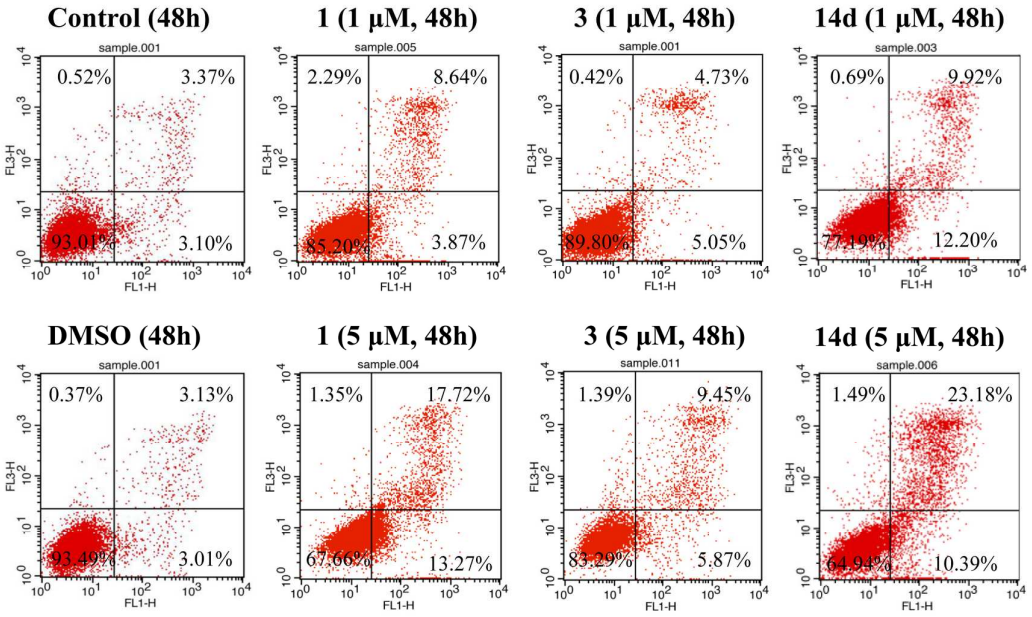

Figure 7. Effects of compounds **1**, **3** and **14d** on the induction of apoptosis in A549 cells. The cells were exposed to increasing concentrations of each compound for 48 h and analyzed by annexin V/propidium iodide double staining. The data are representative of two independent experiments.

Biological Activity of Enantiomers of Compound 14d. The enantiomers of compound **14d** were separated by chiral column chromatography and tested the optical rotation by polarimeter. Furthermore, the configuration of enantiomers of **14d** could be identified by the comparison of optical rotation to that of enantiomers of **3** (**Figure 8A** and **Supporting Information Figure S2**). Fluorescence polarization binding assay revealed that their MDM2 inhibitory activities were significantly different **(Figure 8B)**. Enantiomers **14d-2** (K_i = 0.06 μM) was about 180-fold more potent than enantiomer **14d-1** (K_i = 10.89 μM). Furthermore, Western blotting was used to verify the MDM2 inhibitory activity of enantiomers **14d-1** and **14d-2** in A549 cells. Consistent with the fluorescence polarization binding assay, enantiomer **14d-2** significantly increased the level of p53 and up-regulated the expression of MDM2 via negative feedback loop after 12 h, whereas enantiomer **14d-1** caused the increase of p53 only at the high concentration (10 μM) **(Figure 8C)**.

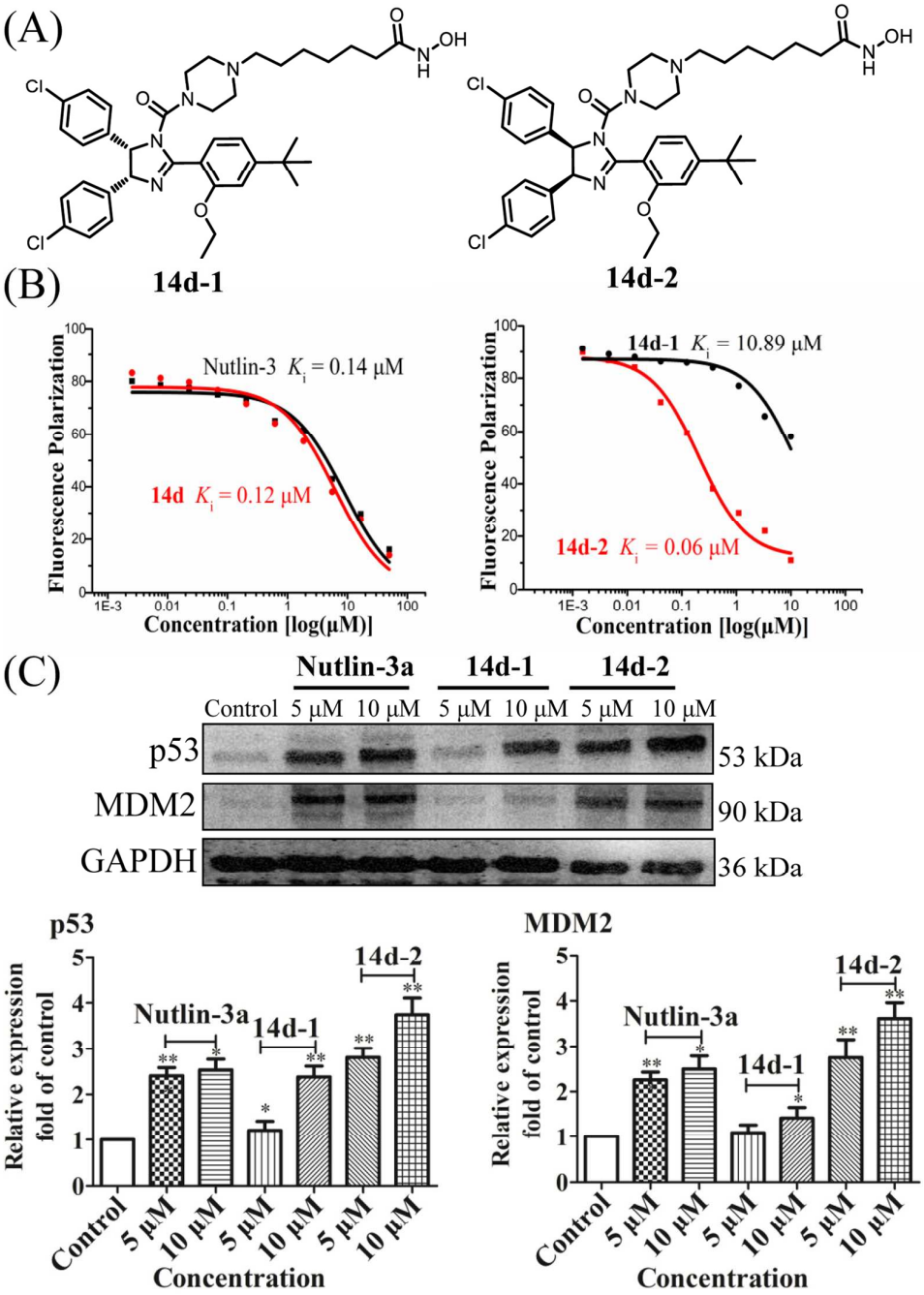

Figure 8. MDM2 inhibitory activities of compound **14d** enantiomers. (A) Chemical structures of compound **14d** enantiomers, which were separated by chiral column chromatography. (B) The MDM2 binding affinity of compound **14d** enantiomers. (C) Effects of compounds on the level of p53 and MDM2 in A549 cells using the Western blotting analysis. GAPDH was used as the loading control. Quantitative analysis of

Western blotting was performed with ImageQuant. Data were presented as means ± SEM, n = 3. * $P < 0.05$ and ** $P < 0.01$ *vs* control group.

Subsequently, HDAC1 inhibitory activity of compounds **14d-1** and **14d-2** were evaluated **(Table 5)**. Interestingly, enantiomer **14d-1** (IC_{50} = 0.91 μM) showed similar activity to enantiomer **14d-2** (IC_{50} = 0.89 μM). The results indicated that the chiral centers on the imidazole scaffold had significant impact on the binding of the two 4-chloropnenyl groups with MDM2 hot spots. In contrast, as the cap group, the conformation of 4-chloropnenyl groups had little effect on HDAC1 binding. Consistently, enantiomer **14d-2** showed better antiproliferative activity than **14d-1**. The different antiproliferative activity of two enantiomers also indirectly revealed that simultaneously inhibited HDAC and MDM2 by a single-molecule were capable of generating synergistic antitumor activities.

Table 5. Biological Activities of Enantiomers of 14d[a]

Compound	p53-MDM2 (K_i, μM)	IC_{50} (μM)		
		HDAC1	HCT116	A549
14d-1	10.89 ± 1.12	0.91 ± 0.08	10.03 ± 0.93	9.02 ± 0.47
14d-2	0.06 ± 0.01	0.89 ± 0.12	1.11 ± 0.24	0.99 ± 0.12
3	0.14 ± 0.03	＞100	9.97 ± 0.86	9.58 ± 0.63

[a] K_i and IC_{50} values are the mean of at least three independent assays, presented as mean ± SD.

Binding Mode of Enantiomers of Compound 14d with MDM2 and HDAC1. To investigate the binding mode of enantiomers of compound **14d** with MDM2 and HDAC1, computational docking studies were performed. As shown in **Figure 9A**, **14d-2** mimicked the interactions of p53 binding site on MDM2. Three aromatic substituents of the scaffolds projected into the pockets normally occupied by the three key residues (Phe19, Trp23, and Leu26) of p53. Ethyl ether side chain in **14d-2** directed toward the Phe19 pocket, the two 4-chlorophenyl groups of **14d-2** projected into the Leu26 and the Trp23 pocket, respectively. Moreover, the 4-chlorophenyl moiety formed π-π stacking interaction with His92 (**Figure 9A and Figure S3A** in **Supporting Information**). In contrast, the ethyl ether side chain of **14d-1** was located at the outside of the Phe19 pocket (**Figure 9C**) and the hydrophobic interactions were lost (**Figure 9C and Figure S3C** in **Supporting Information**). It might be the main reason why the MDM2 binding affinity of **14d-1** was inferior to that of **14d-2**.

The binding mode of enantiomers of compound **14d** with HDAC1 was shown in **Figure 9B** and **9D**. Compound **14d-1** and **14d-2** bound with HDAC1 mainly through the linker and ZBG. The aliphatic linker was projected into the hydrophobic cavity of HDAC1. Besides chelating with Zn^{2+}, the terminal hydroxamic acid group of **14d-2** formed two hydrogen bonds with Tyr308 and His145, respectively. Moreover, the 4-chloropnenyl group in the cap formed π-π stacking interactions with Arg275 (**Figure 9B** and **Figure S3B** in **Supporting Information**). Similarly, the hydroxamic acid group of **14d-1** chelated with Zn^{2+} and formed two hydrogen bonds with Gly143 and His145, respectively. In addition, hydrogen bonding interaction was observed

between the carbonyl group of **14d-1** and Phe210 (**Figure 9D** and **Figure S3D** in **Supporting Information**). The computational docking result was consistent with the fact that the two enantiomers had similar HDAC1 inhibitory activity.

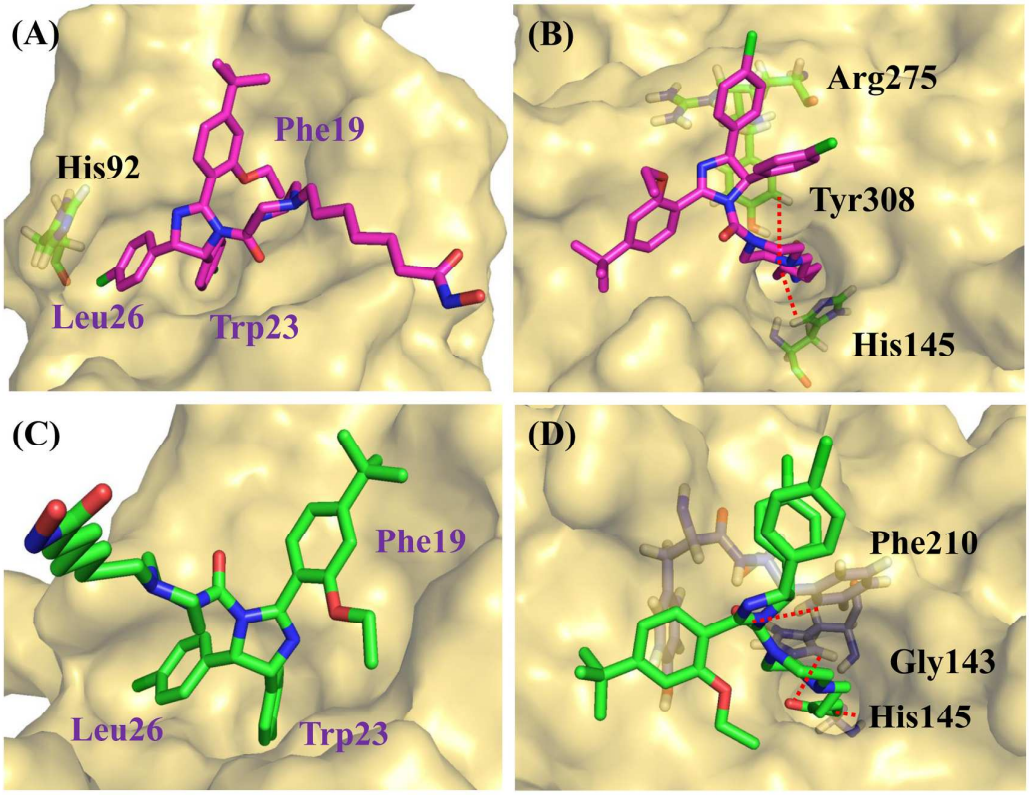

Figure 9. The binding modes of compound 14d enantiomers with MDM2 and HDAC1. (A) Compound **14d-2** (red) projected into the three hot spots of MDM2 (PDB ID: 4IPF). (B) Proposed binding mode of **14d-2** (red) in the active site of HDAC1 (PDB ID: 4BKX). (C) Binding mode of compound **14d-1** (green) with MDM2 (PDB ID: 4IPF). The ethyl ether was buried out the Phe19 pocket. (D) Proposed binding mode of **14d-1** (green) in the active site of HDAC1 (PDB ID: 4BKX). The figure was generated using PyMol. (http://www.pymol.org/).

***In vivo* Antitumor Efficacy of Compound 14d.** Compound **14d** was evaluated for *in vivo* antitumor effcacy in the A549 xenograft nude mouse model. When tumors had reached an average volume of 100 mm^3 in the 11th day after implantation, compound **14d** was administered orally (po) at 100 mg/kg/day and 150 mg/kg/day for 21 consecutive days, respectively. Compounds **1** (100 mg/kg/day, po) and **3** (100 mg/kg/day, po) were used as the positive controls. As shown in **Figure 10**, compound **14d** effectively inhibited the tumor growth in a dose-dependent manner compared to the vehicle control. Oral administration of 100 mg/kg/day of compound **14d** achieved the tumor growth inhibition (TGI) of 65.4%. At 150 mg/kg/day, the TGI of compound **14d** was increased to 74.5%, whose *in vivo* potency was better than compound **1** (100 mg/kg/day, TGI = 57.3%) ($P < 0.01$) and **3** (100 mg/kg/day, TGI = 44.0%) ($P < 0.01$). Notably, no significant body weight loss and no adverse effects were observed for compound **14d** during the *in vivo* studies. The results highlighted the advantages of dual inhibition of MDM2 and HDAC for the treatment of A549 lung cancer.

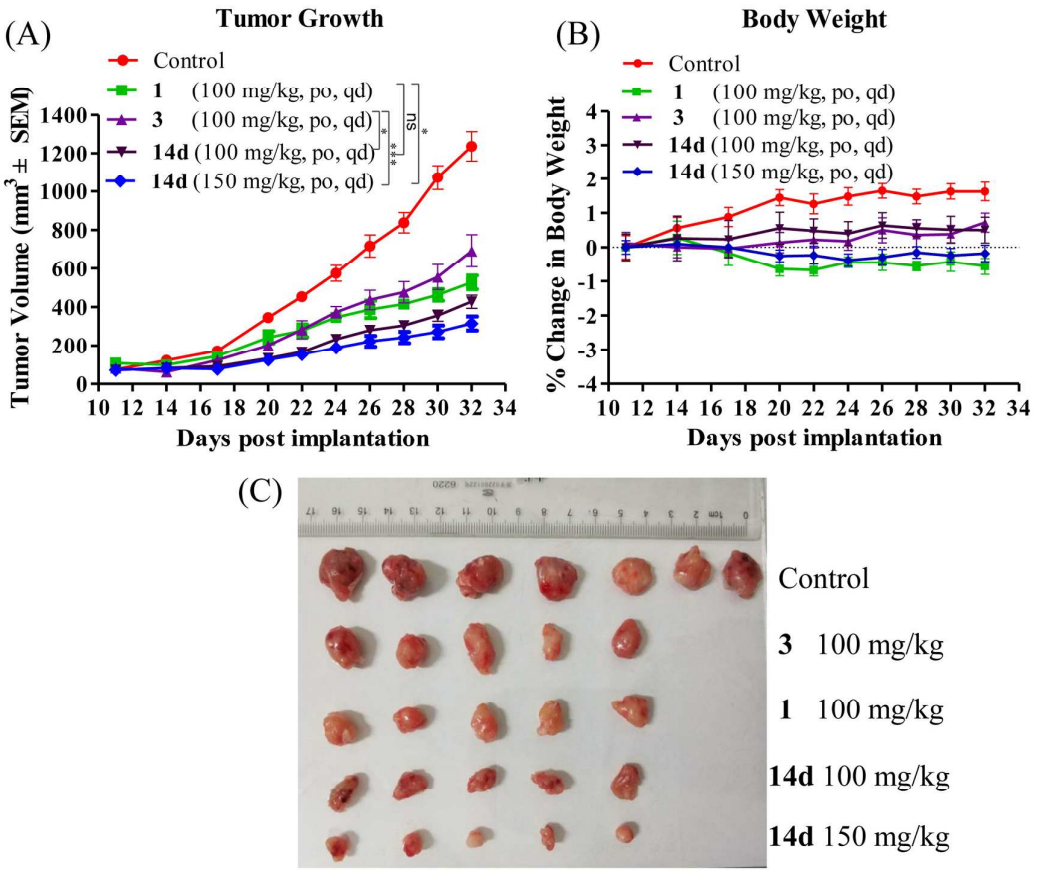

Figure 10. *In vivo* antitumor potency of compound **14d**. (A) Antitumor activity of compound **14d**, in comparison to compounds **1** and **3**, in the A549 lung cancer xenograft model in nude mice. Compound **14d** was treated with oral gavage at 100 or 150 mg/kg daily for 21 days and reference compounds was treated with oral gavage at 100 mg/kg once per day for 21 days. The antitumor potency was expressed by TGI. TGI was calculated according to the formula, TGI = (1- tumor volume of treatment group/ tumor volume of control group) × 100%, at the end of treatment. Data are expressed as the mean ± standard deviation. * $P < 0.05$ and *** $P < 0.001$, determined with 1-way ANOVA test for significance. (B) Changes in body weight of mice during treatment period. (C) The picture of dissected A549 tumor tissues.

Preliminary Pharmacokinetic (PK) Profiles of Compound 14d. Given the encouraging biological profile and xenograft efficacy, PK profiles of **14d** were evaluated in Sprague-Dawley (SD) rats. Compound **14d** was administered intravenously (IV) and orally (Po) at 5 mg/kg and 20 mg/kg, respectively. As summarized in **Table 6**, the half-life, peak concentration (C_{max}) and plasma clearance (CL) of **14d** were 1.22 h, 1470.7 ng/mL and 2809.1 mL/h/mg, respectively. After oral administration, **14d** exhibited reasonable PK properties in rats with oral bioavailabilty of 18% and showed significant improvement $T_{1/2}$ with 5.87 h.

Table 6. Pharmacokinetic Parameters of 14d in SD Rats[α]

PK parameters	IV 2 mg/kg	Po 20 mg/kg
$T_{1/2}$ (h)	1.22 ± 0.12	5.87 ± 0.34
T_{max} (h)	0.083 ± 0.00	3.33 ± 1.15
C_{max} (ng/mL)	1470.70 ± 88.50	93.71 ± 23.32
$AUC_{0-\infty}$ (h*ng/mL)	716.3 ± 68.1	323.23 ± 39.01
V_{ss} (mL/mg)	4901.0 ± 33.9	
CL (mL/h/mg)	2809.1 ± 269.5	
F (%)		18

[α]C_{max}, maximum concentration of the compound detected in plasma; AUC, area under the curve; $T_{1/2}$, terminal half-life; T_{max}, peak time; CL, apparent total body clearance of the drug from plasma; V_{ss}, volume distribution; F, oral bioavailability.

CONCLUSIONS

In summary, novel MDM2/HDACs dual inhibitors were identified on the basis of the pharmacophore fusion strategy. Several dual inhibitors showed excellent activities towards both targets. Particularly, compound **14d** revealed potent activities at both molecular and cellular level. Antitumor mechanism studies indicated that compound **14d** acted by activating p53 and increasing the H3, H4 and α-tubulin acetylation in A549 cancer cells. It significantly induced the apoptosis of A549 cells with a G0/G1 cell cycle arrest. Compound **14d** was orally active and exhibited excellent *in vivo* antitumor potency in the A549 xenograft model (TGI = 74.5%), which was much more effective than HDAC inhibitor **1** and MDM2 inhibitor **3**. The results highlighted the advantages of dual MDM2/HDAC inhibitors as a promising strategy for multi-targeting antitumor drug discovery. Further antitumor mechanism and structural optimization studies are in progress.

EXPERIMENTAL SECTION

Chemistry. Unless otherwise noted, all reagents were obtained from commercial suppliers and used without further purification. All starting materials were commercially available. ^{1}H NMR and ^{13}C NMR spectra were recorded on Bruker AVANCE300 and AVANCE600 spectrometer (Bruker Company, Germany), using TMS as an internal standard and DMSO-d_6 as solvents. Chemical shift is given in ppm (δ). The mass spectra were recorded on an Esquire 3000 LC-MS mass spectrometer. TLC analysis was carried out on silica gel plates GF254 (Qingdao

Haiyang Chemical, China). Silica gel column chromatography was performed with Silica gel 60 G (Qingdao Haiyang Chemical, China). Chemical purities were analyzed by HPLC using hexane/2-propanol as the mobile phase with a flow rate of 0.8 mL/min on an AD-H column. All final compounds exhibited the purity greater than 95%.

2-(4-(*Tert*-butyl)-2-ethoxyphenyl)-4,5-bis(4-chlorophenyl)-4,5-dihydro-1*H*-imidazole (7). Intermediates 4-(*tert*-butyl)-2-ethoxybenzoic acid (**5**),[56] (1*R*,2*S*)-1,2-bis(4-chlorophenyl)ethane-1,2-diamine (**6**)[62] were prepared according to the literature. A mixture of **5** (1.04 g, 3.70 mmol), **6** (0.90 g, 4.07 mmol), and boric acid (22.9 mg, 0.37 mmol) in xylenes (15 mL) was stirred at 145 ^{o}C for 8 h. Then, the solvent was removed by distillation. The residual was diluted with EtOAc (100 mL), washed with saturated NaCl solution (30 mL), and saturated $NaHCO_3$ solution (30 mL), then dried over anhydrous Na_2SO_4. The organic phase was evaporated under reduced pressure to give yellow oil, which was purified by silica gel column chromatography (EtOAc: MeOH = 95: 5) to obtain compound **7** (1.29 g, 70%) as a yellow solid. ^{1}H NMR (DMSO-d_6, 300 MHz) δ: 1.37 (s, 9H), 1.43 (t, J = 6.76 Hz, 3H), 4.34 (dd, J = 7.21 Hz, 6.21 Hz, 2H), 5.86 (s, 2H), 7.11 (d, J = 8.11 Hz, 4H), 7.25 (d, J = 8.71 Hz, 6H), 7.90 (d, J = 7.81 Hz, 1H), 10.40 (s, 1H). ESI-MS (m/s): 467.54 $[M + H]^+$.

2-(4-(*Tert*-butyl)-2-ethoxyphenyl)-4,5-bis(4-chlorophenyl)-4,5-dihydro-1*H*-imidazole-1-carbonyl chloride (8). To a stirred solution of triphosgene (0.11 g, 0.35 mmol) in CH_2Cl_2 (5 mL) was added dropwise a solution of compound **7** (0.50 g, 1.05

mmol) and Et_3N (0.30 mL, 2.1 mmol) in CH_2Cl_2 (5 mL) at 0 °C over 30 min. The resulting mixture was warmed to room temperature and stirred for 1 h. Then, 1 N HCl solution (10 mL) was added dropwise to the mixture. After separation, the aqueous phase was extracted with CH_2Cl_2 (3 × 5 mL). The combined organic phases were washed with saturated $NaHCO_3$ solution and saturated NaCl solution (3 × 5 mL), then dried over anhydrous Na_2SO_4. After removal of the solvent, the crude product was purified by silica gel column chromatography (Hexane: EtOAc = 10: 1) to afford compound **8** (0.36 g, 65%) as a white solid. ^{1}H NMR (DMSO-d_6, 600 MHz) δ: 1.37 (s, 9H), 1.43 (t, J = 6.94 Hz, 3H), 4.03-4.17 (m, 1H), 4.273-4.40 (m, 1H), 5.72 (d, J = 9.63 Hz, 1H), 5.78 (d, J = 9.63 Hz, 1H), 6.94 (s, 1H), 6.96 (s, 1H), 7.00 (s, 1 H), 7.05-7.10 (d, J = 8.10 Hz, 3H), 7.10-7.17 (m, 4H), 7.57 (d, J = 7.92 Hz, 1H).

Methyl-5-(2-(4-(*tert*-butyl)-2-ethoxyphenyl)-4,5-bis(4-chlorophenyl)-4,5-dihydro-1*H*-imidazole-1-carboxamido)pentanoate (10a). To a solution of **9a** (0.18 g, 1.35 mmol) was added Et_3N (0.32 mL, 2.28 mmol), followed by dropwise addition of **8** (0.60 g, 1.14 mmol) in CH_2Cl_2 (5 mL). The solution was stirred for 1 h at room temperature, then it was washed successively with 2 N HCl (5 mL) solution, 10% $NaHCO_3$ (5 mL) and water, dried over anhydrous Na_2SO_4, filtered and the solvent was then evaporated to give the impure amide which was purified by silica gel column chromatography (CH_2Cl_2: MeOH = 100: 1) to give compound **10a** (0.63 g, 85%) as a white solid. ^{1}H NMR (DMSO-d_6, 300 MHz) δ: 1.22-1.34 (m, 5H), 1.33 (s, 9H), 2.11 (t, J = 6.75 Hz, 2H), 2.21 (t, J = 5.52 Hz, 2H), 2.90-3.81 (m, 2H), 3.56 (s, 3H), 4.12-4.24 (m, 1H), 4.30-4.41 (m, 1H), 5.31 (s, 1H), 5.78 (dd, J = 10.76 Hz, 6.52

Hz, 2H), 7.02-7.13 (m, 4H), 7.15-7.19 (m, 6H), 7.41 (d, J = 6.28 Hz, 1H).

Compounds **10b-10d**, **18**, **20a-e, 21a-b, 22a-b** and **23** were synthesized according to a similar procedure described for **10a.**

***N*-(5-((2-aminophenyl)amino)-5-oxopentyl)-2-(4-(*tert*-butyl)-2-ethoxyphenyl)-4, 5-bis(4-chlorophenyl)-4,5-dihydro-1*H*-imidazole-1-carboxamide (11a).** To a solution of compound **10a** (0.50 g, 0.80 mmol) in MeOH (5 mL) at 0 ^{o}C was slowly added 2 N LiOH (2 mL) solution over 15 min. The reaction mixture was warmed to room temperature and stirred overnight. Then, the organic solvent was removed under the reduced pressure and the residual aqueous solution was acidified to pH = 2 with 2 N HCl solution to afford the white precipitate. The precipitate was filtered and the filter cake was washed with water for 3 times to give nutlin carboxyl acid. The crude product was used directly in the next step without further purification. The nutlin carboxyl acid (0.20 g, 0.33 mmol), *o*-phenylenediamine (0.039 g, 0.036 mmol) and Et_3N (0.12 mL, 0.83 mmol) were dissolved in DMF (5 mL), and HBTU (0.19g, 0.50 mmol) was added to the solution. After stirring for 30 min, saturated NaCl solution (100 mL) was then added and the mixture was extracted with EtOAc (3×10 mL). The combined organic layers were washed with 2 N HCl (10 mL) solution, H_2O (50 mL), 5% $NaHCO_3$ solution (10 mL), and then H_2O (50 mL), dried over anhydrous Na_2SO_4, filtered, and concentrated under the reduced pressure to give the crude product. The crude product was purified by silica gel column chromatography (CH_2Cl_2: MeOH = 100: 3) to afford compound **11a** (0.18 g, 78.9%) as a white solid. ^{1}H NMR (DMSO-d_6, 600 MHz) δ: 1.25-1.34 (m, 4H), 1.31 (t, J = 6.93 Hz, 3H), 1.33 (s, 9H), 2.16 (t, J =

7.29 Hz, 2H), 2.85 (dd, J = 12.42 Hz, 6.48 Hz, 2H), 3.07-3.12 (m, 1H), 4.02-4.08 (m, 1H), 4.20-4.25 (m, 1H), 4.78 (s, 2H), 5.67 (d, J = 10.26 Hz, 1H), 5.71 (d, J = 10.26 Hz, 1H), 6.50-6.55 (m, 1H), 6.70 (dd, J = 7.76 Hz, 1.11 Hz, 1H), 6.86-6.89 (m, 1H), 7.01-7.05 (m, 4H), 7.09-7.15 (m, 7H), 7.41 (d, J = 7.76 Hz, 1H), 8.98 (s, 1H). ^{13}C NMR (DMSO-d_6, 600 MHz) δ: 9.1, 15.2, 22.7, 29.2, 31.5, 35.3, 35.7, 46.3, 55.4, 64.1, 66.2, 71.9, 109.3, 116.3, 116.6, 117.2, 124.0, 125.6, 126.1, 127.7, 129.6, 130.3, 131.4, 131.8, 137.1, 138.2, 142.2, 152.3, 154.8, 156.9, 159.7, 171.3. HRMS m/z calcd for $C_{39}H_{43}Cl_2N_5O_3$ $[M + H]^+$ 700.2816, found 700.2838. HPLC purity 95.5%. Retention time: 13.4 min, eluted with 9% n-hexane/91% isopropanol.

Target compounds **11b-d** were synthesized according to a similar procedure described for **11a.**

***N*-(6-((2-Aminophenyl)amino)-6-oxohexyl)-2-(4-(tert-butyl)-2-ethoxyphenyl)-4, 5-bis(4-chlorophenyl)-4,5-dihydro-1*H*-imidazole-1-carboxamide (11b).** The product was obtained as a white solid (0.30 g, 0.42 mmol), yield: 81.1%. ^{1}H NMR (DMSO-d_6, 600 MHz) δ: 1.10-1.19 (m, 4H), 1.32 (t, J = 6.95 Hz, 3H), 1.34 (s, 9H), 1.37-1.42 (m, 2H), 2.19 (t, J = 7.45 Hz, 2H), 2.78-2.90 (m, 2H), 4.01-4.07 (m, 1H), 4.07-4.11 (m, 1H), 4.78 (s, 2H), 5.66 (d, J = 10.43 Hz, 1H), 5.71 (d, J = 10.43 Hz, 1H), 5.94 (s, 1H), 6.53 (t, J = 6.95 Hz, 1H), 6.70 (d, J = 7.95 Hz, 1H), 6.88 (t, J = 6.95 Hz, 1H), 7.01-7.05 (m, 4H), 7.10-7.13 (m, 7H), 7.39 (d, J = 7.95 Hz, 1H), 9.02 (s, 1H). ^{13}C NMR (DMSO-d_6, 600 MHz) δ: 9.2, 14.6, 15.2, 21.2, 25.3, 26.1, 29.3, 31.5, 35.3, 36.0, 46.3, 60.2, 64.1, 66.2, 72.0, 109.4, 116.4, 116.7, 117.1, 119.8, 124.0, 125.7, 126.1, 127.7, 127.8, 129.6, 130.2, 130.3, 131.4, 131.9, 137.2, 138.3, 142.3,

152.3, 154.7, 156.9, 159.7, 171.5. HRMS m/z calcd for $C_{40}H_{45}Cl_2N_5O_3$ $[M + H]^+$ 714.2972, found 714.2939. HPLC purity 96.2%. Retention time: 12.5 min, eluted with 10% n-hexane/90% isopropanol.

***N*-(7-((2-Aminophenyl)amino)-7-oxoheptyl)-2-(4-(tert-butyl)-2-ethoxyphenyl)-4,5-bis(4-chlorophenyl)-4,5-dihydro-1*H*-imidazole-1-carboxamide (11c).** The product was obtained as a pale white solid (0.19 g, 0.26 mmol), yield: 75.2%. ^{1}H NMR (DMSO-d_6, 600 MHz) δ: 0.89-0.93 (m, 2H), 1.08-1.17 (m, 4H), 1.32 (t, J = 7.02 Hz, 3H), 1.34 (s, 9H), 1.44-1.47 (m, 2H), 2.23 (t, J = 7.27 Hz, 2H), 2.76-2.80 (m, 1H), 2.85-2.90 (m, 1H), 4.03-4.08 (m, 1H), 4.20-4.22 (m, 1H), 4.85 (s, 2H), 5.67 (d, J = 10.53 Hz, 1H), 5.73 (d, J = 10.53 Hz, 1H), 5.97 (s, 1H), 6.53 (t, J = 7.52 Hz, 1H), 6.71 (d, J = 7.77 Hz, 1H), 6.89 (t, J = 7.52 Hz, 1H), 7.04 (t, J = 7.57 Hz, 4H), 7.09-7.15 (m, 7H), 7.41 (d, J = 7.77 Hz, 1H), 9.04 (s, 1H). ^{13}C NMR (DMSO-d_6, 600 MHz) δ: 15.2, 25.6, 26.3, 28.8, 29.4, 31.5, 35.3, 36.2, 46.2, 55.4, 64.1, 66.2, 71.8, 109.3, 116.4, 116.7, 117.2, 119.6, 124.1, 125.7, 126.1, 127.7, 127.8, 129.6, 130.2, 130.3, 131.5, 31.9, 137.2, 138.2, 142.3, 152.2, 154.8, 156.9, 159.8, 171.5. HRMS m/z calcd for $C_{41}H_{47}Cl_2N_5O_3$ $[M + H]^+$ 728.3129, found 728.3136. HPLC purity 97.1%. Retention time: 12.2 min, eluted with 10% n-hexane/90% isopropanol.

***N*-(8-((2-aminophenyl)amino)-8-oxooctyl)-2-(4-(*tert*-butyl)-2-ethoxyphenyl)-4,5-bis(4-chlorophenyl)-4,5-dihydro-1*H*-imidazole-1-carboxamide (11d).** The product was obtained as a pale white solid (0.23 g, 0.31 mmol), yield: 79.0%. ^{1}H NMR (DMSO-d_6, 600 MHz) δ: 0.84-0.89 (m, 2H), 1.07-1.12 (m, 4H), 1.15-1.20 (m, 2H), 1.32 (t, J = 6.94 Hz, 3H), 1.34 (s, 9H), 1.48-1.54 (m, 2H), 2.27 (t, J = 7.32 Hz, 2H),

2.74-2.78 (m, 1H), 2.85-2.91 (m, 1H), 4.02-4.07 (m, 1H), 4.18-4.22 (m, 1H), 4.80 (s, 2H), 5.66 (d, J = 7.48 Hz, 1H), 5.71 (d, J = 7.48 Hz, 1H), 5.93 (s, 1H), 6.53 (t, J = 7.28 Hz, 1H), 6.71 (d, J = 8.19 Hz, 1H), 6.88 (d, J = 7.74 Hz, 1H), 7.01-7.03 (m, 4H), 7.08-7.13 (m, 7H), 7.39 (d, J = 7.74 Hz, 1H), 9.07 (s, 1H); ^{13}C NMR (DMSO-d_6, 600 MHz) δ: 15.2, 25.7, 26.4, 29.0, 29.0, 29.4, 30.1, 31.5, 35.3, 36.2, 56.3, 64.1, 64.3, 66.1, 68.9, 71.9, 109.3, 116.4, 116.6, 117.1, 119.9, 124.1, 125.7, 126.1, 127.7, 127.8, 129.6, 130.2, 130.3, 131.40, 131.9, 137.2, 138.3, 142.3, 152.2, 154.6, 156.8, 159.7, 171.6. HRMS m/z calcd for $C_{42}H_{49}Cl_2N_5O_3$ $[M + H]^+$ 742.3285, found 742.3297. HPLC purity 96.5%. Retention time: 12.7 min, eluted with 10% n-hexane/90% isopropanol.

2-(4-(*Tert*-butyl)-2-ethoxyphenyl)-4,5-bis(4-chlorophenyl)-*N*-(5-(hydroxyamino)-5-oxopentyl)-4,5-dihydro-1*H*-imidazole-1-carboxamide (12a). To a stirred solution of hydroxylamine hydrochloride (4.67 g, 67 mmol) in MeOH (24 mL) was added dropwise a solution of KOH (5.61 g, 100 mmol) in MeOH (12 mL) at 0 °C. Then, the mixture was stirred for 30 min at 0 °C. The precipitate was filtered and the filtrate formed a solution of free hydroxylamine in MeOH. Subsquently, compound **10a** (0.1 g, 0.16 mmol) was dissolved in 5 mL of the above freshly prepared MeOH solution of hydroxylamine. The mixture was stirred at room temperature for 1 h, and then adjusted to pH = 7 with 2 N HCl. The mixture was concentrated and the residue was washed with water to afford crude product. For an accurate yield the crude product was purified by recrystallization and afforded compound **12a** (0.91 g, 90%) as a white solid. ^{1}H NMR (DMSO-d_6, 600 MHz) δ: 1.05-1.11 (m, 2H), 1.12-1.20 (m,

2H), 1.33 (s, 9H), 1.34 (t, J = 9.10 Hz, 3H), 1.76 (t, J = 7.48 Hz, 2H), 2.78-2.86 (m, 2H), 3.17 (s, 1H), 4.09-4.13 (m, 1H), 4.20-4.24 (m, 1H), 5.81 (d, J = 8.72 Hz, 1H), 5.94 (d, J = 8.72 Hz, 1H), 7.06-7.12 (m, 6H), 7.15-7.18 (m, 4H), 7.50 (d, J = 6.23 Hz, 1H), 8.61 (s, 1H), 10.28 (s, 1H); ^{13}C NMR (DMSO-d_6, 600 MHz) δ: 15.1, 22.6, 28.8, 29.1, 30.2, 31.4, 32.2, 35.5, 49.1, 64.4, 64.6, 109.6, 117.4, 120.2, 128.0, 128.9, 129.6, 129.7, 130.2, 130.5, 136.2, 138.2, 151.2, 153.3, 156.9, 158.9, 169.2. HRMS m/z calcd for $C_{33}H_{38}Cl_2N_4O_4$ [M - H]$^-$ 623.2197, found 623.2182. HPLC purity 96.1%. Retention time: 15.1 min, eluted with 8% n-hexane/92% isopropanol.

Target compounds **12b-17** were synthesized according to a similar procedure described for **12a.**

2-(4-(*Tert*-butyl)-2-ethoxyphenyl)-4,5-bis(4-chlorophenyl)-*N*-(6-(hydroxyamino)-6-oxohexyl)-4,5-dihydro-1*H*-imidazole-1-carboxamide (12b). The product was obtained as a white solid (0.20 g, 0.31 mmol), yield: 90.7%. ^{1}H NMR (DMSO-d_6, 600 MHz) δ: 0.81-0.91 (m, 2H), 1.02-1.12 (m, 2H), 1.21-1.31 (m, 2H), 1.35 (t, J = 10.27 Hz, 3H), 1.36 (s, 9H), 1.82 (t, J = 6.69 Hz, 2H), 2.00 (s, 1H), 2.72-2.82 (m, 1H), 2.83-2.93 (m, 1H), 4.11 (t, J = 8.03 Hz, 1H), 4.23 (t, J = 8.03 Hz, 1H), 5.79 (s, 1H), 5.89 (s, 1H), 7.08-7.11 (m, 4H), 7.12 (d, J = 6.60 Hz, 2H), 7.17 (d, J = 7.59 Hz, 4H), 7.49 (s, 1H), 8.64 (s, 1H), 10.32 (s, 1H); ^{13}C NMR (DMSO-d_6, 600 MHz) δ: 15.1, 21.2, 25.2, 26.1, 29.0, 31.1, 31.5, 32.5, 35.4, 60.2, 64.3, 66.4, 109.5, 117.3, 120.1, 127.9, 129.0, 129.7, 129.8, 130.3, 130.4, 136.5, 137.6, 151.1, 153.3, 156.9, 158.9, 169.4. HRMS m/z calcd for $C_{34}H_{40}Cl_2N_4O_4$ [M + H]$^+$ 639.2499, found 639.2431. HPLC purity 96.9%. Retention time: 14.5 min, eluted with 10% n-hexane/90%

isopropanol.

2-(4-(*tert*-butyl)-2-ethoxyphenyl)-4,5-bis(4-chlorophenyl)-*N*-(7-(hydroxyamino)-7-oxoheptyl)-4,5-dihydro-1*H*-imidazole-1-carboxamide (12c). The product was obtained as a white solid (0.11 g, 0.17 mmol), yield: 86.7%. ^{1}H NMR (DMSO-d_6, 600 MHz) δ: 0.85-0.88 (m, 2H), 1.01-1.67 (m, 4H), 1.30-1.33 (m, 5H), 1.33 (s, 9H), 1.86 (d, J = 7.28Hz, 2H), 2.73-2.77 (m, 1H), 2.82-2.88 (m, 1H), 4.02-4.09 (m, 1H), 4.20-4.23 (m, 1H), 5.66 (d, J = 10.32 Hz, 1H), 5.71 (d, J = 10.32 Hz, 1H), 5.90 (s, 1H), 7.00-7.04 (m, 4H), 7.09-7.14 (m, 6H), 7.39 (d, J = 7.60 Hz, 1H), 8.61 (s, 1H), 10.26 (s, 1H); ^{13}C NMR (DMSO-d_6, 600 MHz) δ: 14.7, 24.9, 25.7, 28.2, 28.8, 31.0, 32.2, 34.8, 63.6, 65.7, 71.5, 108.9, 116.7, 119.4, 127.2, 127.3, 129.1, 129.7, 129.8, 130.9, 131.4, 136.8, 137.8, 151.8, 154.2, 156.4, 159.1, 169.0. HRMS m/z calcd for $C_{35}H_{42}Cl_2N_4O_4$ $[M + H]^+$ 653.2656, found 653.2623. HPLC purity 95.8%. Retention time: 13.3 min, eluted with 10% n-hexane/90% isopropanol.

2-(4-(*Tert*-butyl)-2-ethoxyphenyl)-4,5-bis(4-chlorophenyl)-N-(8-(hydroxyamino)-8-oxooctyl)-4,5-dihydro-1*H*-imidazole-1-carboxamide (12d). The product was obtained as a white solid (0.09 g, 0.13 mmol), yield: 85.9%. ^{1}H NMR (DMSO-d_6, 600 MHz) δ: 0.65-0.95 (m, 4H), 0.92-1.20 (m, 6H), 1.33 (s, 9H), 1.34 (t, J = 10.63 Hz, 3H), 1.88 (s, 2H), 2.75 (s, 1H), 2.86 (s, 1H), 4.05 (s, 1H), 4.20 (s, 1H), 5.72 (d, J = 10.03 Hz, 1H), 5.78 (d, J = 10.03 Hz, 1H), 6.20 (s, 1H), 6.99-7.19 (m, 10H), 7.41 (d, J = 6.57 Hz, 1H), 8.65 (s, 1H), 10.33 (s, 1H); ^{13}C NMR (DMSO-d_6, 600 MHz) δ: 15.2, 22.5, 25.5, 26.3, 28.9, 29.4, 31.5, 32.7, 35.3, 64.1, 66.2, 71.5, 109.3, 116.2, 117.2, 119.3, 127.8, 129.6, 130.3, 131.5, 131.9, 137.1, 137.7, 151.9, 155.0, 156.9, 160.0,

169.5. HRMS m/z calcd for $C_{36}H_{44}Cl_2N_4O_4$ $[M + H]^+$667.2812, found 667.2819. HPLC purity 95.9%. Retention time: 12.9 min, eluted with 10% n-hexane/90% isopropanol.

2-(4-(*Tert*-butyl)-2-ethoxyphenyl)-4,5-bis(4-chlorophenyl)-*N*-(4-(hydroxycarbamoyl)benzyl)-4,5-dihydro-1*H*-imidazole-1-carboxamide (13). The product was obtained as a white solid (0.37 g, 0.56 mmol), yield: 92.4%. ^{1}H NMR (DMSO-d_6, 600 MHz) δ: 1.26 (t, J = 6.91 Hz, 3H), 1.31 (s, 9H), 3.90-4.07 (m, 2H), 4.15 (dd, J = 9.55 Hz, 5.55Hz, 2H), 5.72 (d, J = 10.37 Hz, 1H), 5.78 (d, J = 10.37 Hz, 1H), 6.78 (s, 1H), 6.90 (d, J = 7.57 Hz, 2H), 6.95-7.05(m, 4H), 7.13 (d, J = 8.89 Hz, 6H), 7.38 (d, J = 8.23 Hz, 1H), 7.53 (d, J = 8.07 Hz, 2H), 8.96 (s, 1H), 11.12 (s, 1H); ^{13}C NMR (DMSO-d_6, 600 MHz) δ: 15.2, 31.5, 35.3, 43.2, 63.9, 66.0, 72.2, 109.2, 117.0, 120.0, 126.9, 127.8, 127.8, 129.7, 130.1, 130.3, 131.4, 132.0, 137.0, 138.2, 143.3, 152.4, 154.4, 156.9, 159.8, 164.5. HRMS m/z calcd $C_{36}H_{36}Cl_2N_4O_4$ $[M - H]^-$ 657.2041, found 657.2033. HPLC purity 96.6%. Retention time: 14.6 min, eluted with 10% n-hexane/90% isopropanol.

2-(4-(2-(4-(*Tert*-butyl)-2-ethoxyphenyl)-4,5-bis(4-chlorophenyl)-4,5-dihydro-1*H*-imidazole-1-carbonyl)piperazin-1-yl)-*N*-hydroxyacetamide (14a). The product was obtained as a white solid (0.41 g, 0.63 mmol), yield: 91.6%. ^{1}H NMR (DMSO-d_6, 600 MHz) δ: 1.31 (t, J = 6.97 Hz, 3H), 1.35 (s, 9H), 1.83 (s, 4H), 2.63 (s, 2H), 3.02 (s, 4H), 4.08 (dd, J = 13.88 Hz, 7.22 Hz, 2H), 5.53 (d, J = 10.00 Hz, 1H), 5.67 (d, J = 10.00 Hz, 1H), 6.96 (d, J = 7.78 Hz, 2H), 7.02 (d, J = 8.33 Hz, 2H), 7.06-7.12 (m, 4H), 7.16 (d, J = *8.33* Hz, 2H), 7.50 (d, J = 8.33 Hz, 1H), 8.69 (s, 1H), 10.30 (s, 1H);

^{13}C NMR (DMSO-d_6, 600 MHz) δ: 14.4, 31.1, 34.9, 45.3, 51.8, 59.0, 63.5, 67.9, 70.6, 108.8, 116.9, 117.6, 127.4, 127.4, 128.7, 129.7, 130.2, 131.1, 131.1, 136.5, 137.4, 155.1, 155.1, 156.5, 159.9, 165.4. HRMS m/z calcd for $C_{34}H_{39}Cl_2N_5O_4$ [M + H]$^+$ 652.2452, found 652.2458. HPLC purity 96.1%. Retention time: 29.6 min, eluted with 15% n-hexane/85% isopropanol.

5-(4-(2-(4-(*Tert*-butyl)-2-ethoxyphenyl)-4,5-bis(4-chlorophenyl)-4,5-dihydro-1*H*-imidazole-1-carbonyl)piperazin-1-yl)-*N*-hydroxypentanamide (14b). The product was obtained as a white solid (0.13 g, 0.19 mmol), yield: 89.3%. ^{1}H NMR (DMSO-d_6, 600 MHz) δ: 1.18-1.23 (m, 4H), 1.30 (t, J = 7.01 Hz, 3H), 1.34 (s, 9H), 1.60-1.80 (m, 4H), 1.88 (t, J = 7.01 Hz, 2H), 1.98 (t, J = 6.09 Hz, 2H), 2.90-3.09 (m, 4H), 4.07 (dd, J = 13.40 Hz, 6.07 Hz, 2H), 5.51 (d, J = 10.05 Hz, 1H), 5.66 (d, J = 10.05 Hz, 1H), 6.95 (t, J = 7.92 Hz, 2H), 7.01 (t, J = 8.22 Hz, 2H), 7.04-7.13 (m, 4H), 7.15 (t, J = 8.22 Hz, 2H), 7.50 (d, J = 7.62 Hz, 1H), 8.68 (s, 1H), 10.33 (s, 1H). ^{13}C NMR (DMSO-d_6, 600 MHz) δ: 14.9, 23.4, 26.1, 31.5, 32.5, 35.4, 46.0, 51.9, 57.7, 64.0, 68.4, 70.9, 109.2, 117.5, 117.9, 127.9, 127.9, 129.1, 130.1, 130.7, 131.5, 131.6, 136.9, 137.9, 155.6, 155.6, 157.0, 160.4, 169.5. HRMS m/z calcd for $C_{37}H_{45}Cl_2N_5O_4$ [M + H]$^+$ 694.2921, found 694.2916. HPLC purity 96.5%. Retention time: 28.7 min, eluted with 10% n-hexane/90% isopropanol.

6-(4-(2-(4-(*tert*-butyl)-2-ethoxyphenyl)-4,5-bis(4-chlorophenyl)-4,5-dihydro-1*H*-imidazole-1-carbonyl)piperazin-1-yl)-*N*-hydroxyhexanamide (14c). The product was obtained as a white solid (0.27 g, 0.38 mmol), yield: 90.1%. ^{1}H NMR (DMSO-d_6, 600 MHz) δ: 1.20-1.27 (m, 4H), 1.31 (t, J = 6.95 Hz, 3H), 1.34 (s, 9H), 1.42 (t, J =

6.95 Hz, 2H), 1.52-1.56 (m, 4H), 1.89 (t, *J* = 8.00 Hz, 2H), 1.98 (t, *J* = 6.69 Hz, 2H), 2.99 (s, 4H), 4.04-4.12 (m, 2H), 5.51 (d, *J* = 9.93 Hz, 1H), 5.67 (d, *J* = 9.93 Hz, 1H), 6.95 (d, *J* = 9.93 Hz, 2H), 7.01 (d, *J* = 7.27 Hz, 2H), 7.05-7.13 (m, 4H), 7.15 (d, *J* = 7.90 Hz, 2H), 7.49 (d, *J* = 7.55 Hz, 1H), 8.64 (s, 1H), 10.29 (s, 1H); ^{13}C NMR (DMSO-d_6, 600 MHz) δ: 16.3, 26.8, 27.7, 28.3, 32.9, 34.1, 36.8, 47.4, 53.3, 59.4, 65.4, 69.8, 72.5, 110.6, 118.9, 119.4, 129.3, 129.3, 130.6, 131.6, 132.1, 132.9, 1330, 138.4, 139.3, 156.9, 157.0, 158.4, 161.8, 170.9. HRMS m/z calcd for $C_{38}H_{47}Cl_2N_5O_4$ [M + H]$^+$ 708.3078, found 708.3046. HPLC purity 95.9%. Retention time: 28.2 min, eluted with 10% n-hexane/90% isopropanol.

7-(4-((4*S*,5*R*)-2-(4-(*Tert*-butyl)-2-ethoxyphenyl)-4,5-bis(4-chlorophenyl)-4,5-dihydro-1*H*-imidazole-1-carbonyl)piperazin-1-yl)-*N*-hydroxyheptanamide (14d). The product was obtained as a white solid (0.19 g, 0.26 mmol), yield: 89.4%. ^{1}H NMR (DMSO-d_6, 600 MHz) δ: 1.12-1.20 (m, 4H), 1.22-1.28(m, 4H), 1.31 (t, *J* = 6.81 Hz, 3H), 1.34 (s, 9H), 1.38-1.42(m, 2H), 1.60-1.80(s, 4H), 1.90 (t, *J* = 7.38 Hz, 2H), 3.00 (s, 4H), 4.05-4.10 (m, 2H), 5.52 (d, *J* = 10.12 Hz, 1H), 5.66 (d, *J* = 10.12 Hz, 1H), 6.96 (d, *J* = 7.96 Hz, 2H), 7.02 (d, *J* = 8.36 Hz, 2H), 7.07 (d, *J* = 11.15 Hz, 2H), 7.11 (t, *J* = 8.36 Hz, 2H), 7.15 (d, *J* = 8.36 Hz, 2H), 7.50 (d, *J* = 7.96 Hz, 1H), 8.63 (s, 1H), 10.30 (s, 1H); ^{13}C NMR (DMSO-d_6, 600 MHz) δ: 14.4, 24.9, 26.5, 28.4, 31.0, 32.2, 34.9, 45.5, 51.4, 54.9, 57.5, 63.6, 67.9, 70.6, 108.7, 117.0, 117.5, 127.4, 127.4, 128.6, 129.6, 130.2, 131.0, 131.1, 136.5, 137.4, 155.0, 155.2, 156.5, 159.9, 169.0. HRMS m/z calcd for $C_{39}H_{49}Cl_2N_5O_4$ [M + H]$^+$ 722.3234, found 722.3244. HPLC purity 95.6%. Retention time: 27.8 min, eluted with 10% n-hexane/90% isopropanol.

8-(4-(2-(4-(*tert*-butyl)-2-ethoxyphenyl)-4,5-bis(4-chlorophenyl)-4,5-dihydro-1*H*-imidazole-1-carbonyl)piperazin-1-yl)-*N*-hydroxyoctanamide (14e). The product was obtained as a white solid (0.10g, 0.14 mmol), yield: 84.1%. ^{1}H NMR (DMSO-d_6, 600 MHz) δ: 1.08-1.22 (m, 6H), 1.30 (t, J = 6.51 Hz, 3H), 1.35 (s, 9H), 1.45-1.48 (m, 2H), 1.48-1.50 (s, 2H), 1.93 (t, J = 7.44 Hz, 2H), 2.79 (s, 2H), 3.02 (t, J = 11.17 Hz, 2H), 3.20-3.32(m, 4H), 3.66 (s, 1H), 3.75 (s, 1H), 4.12 (t, J = 6.98 Hz, 1H), 4.19 (t, J = 6.98 Hz, 1H), 5.72 (s, 1H), 5.82 (s, 1H), 7.01 (d, J = 7.91 Hz, 2H), 7.07 (d, J = 7.91 Hz, 2H), 7.15 (t, J = 6.38 Hz, 4H), 7.19 (t, J = 7.18 Hz, 2H), 7.64 (t, J = 7.61 Hz, 1H), 8.67 (s, 1H), 10.37 (s, 1H); ^{13}C NMR (DMSO-d_6, 600 MHz) δ: 14.8, 23.2, 25.4, 26.2, 28.6, 28.7, 31.4, 32.6, 35.6, 42.8, 45.5, 50.6, 52.4, 56.1, 64.4, 68.6, 70.5, 109.5, 117.9, 119.2, 128.1, 129.3, 130.2, 131.3, 132.1, 138.3, 139.3, 155.1, 155.2, 157.0, 159.5, 169.5. HRMS m/z calcd for $C_{40}H_{51}Cl_2N_5O_4$ $[M + H]^+$ 736.3391, found 736.3396. HPLC purity 97.2%. Retention time: 27.1 min, eluted with 10% n-hexane/90% isopropanol.

4-((4-(2-(4-(*tert*-butyl)-2-ethoxyphenyl)-4,5-bis(4-chlorophenyl)-4,5-dihydro-1*H*-imidazole-1-carbonyl)piperazin-1-yl)methyl)-*N*-hydroxybenzamide (15a). The product was obtained as a white solid (0.24 g, 0.33 mmol), yield: 90.9%. ^{1}H NMR (DMSO-d_6, 600 MHz) δ: 1.30 (t, J = 6.35 Hz, 3H), 1.403 (s, 9H), 1.60-1.82(m, 4H), 3.01(s, 4H), 3.25 (dd, J = 9.05 Hz 2H), 4.08 (d, J = 11.67 Hz, 6.42 Hz, 2H), 5.50 (d, J = 10.50 Hz, 1H), 5.66 (d, J = 10.50 Hz, 1H), 6.89-7.05 (m, 4H), 7.06-7.18 (m, 6H), 7.22 (d, J = 7.59 Hz, 2H), 7.50 (d, J = 8.17 Hz, 1H), 7.67 (d, J = 7.59 Hz, 2H), 9.02 (s, 1H), 11.17 (s, 1H); ^{13}C NMR (DMSO-d_6, 600 MHz) δ: 14.9, 31.6, 35.4, 45.9, 51.9,

61.9, 64.0, 68.4, 70.9, 109.2, 117.5, 117.9, 127.3, 127.9, 128.9, 129.1, 130.1, 130.8, 131.5, 131.6, 132.0, 136.9, 137.8, 141.6, 155.5, 155.7, 157.0, 160.4, 164.5. HRMS m/z calcd for $C_{40}H_{43}Cl_2N_5O_4$ [M - H]$^-$ 726.2619, found 726.2617. HPLC purity 97.8%. Retention time: 16.8 min, eluted with 8% n-hexane/92% isopropanol.

2-(4-(2-(4-(*tert*-butyl)-2-ethoxyphenyl)-4,5-bis(4-chlorophenyl)-4,5-dihydro-1*H*-imidazole-1-carbonyl)piperazin-1-yl)-*N*-hydroxypyrimidine-5-carboxamide (15b). The product was obtained as a white solid (0.39 g, 0.55 mmol), yield: 91.8%. ^{1}H NMR (DMSO-d_6, 300 MHz) δ:1.21 (s, 9H), 1.23 (t, J = 15.00 Hz, 3H), 3.08 (s, 4H), 3.20 (s, 4H), 4.10 (d, J = 5.65 Hz, 2H), 5.56 (d, J = 9.35 Hz, 1H), 5.70 (d, J = 9.35 Hz, 1H), 6.98 (d, J = 6.52 Hz, 2H), 7.05 (t, J = 5.98 Hz, 3H), 7.10 (t, J = 7.18 Hz, 3H), 7.17 (d, J = 7.61 Hz, 2H), 7.58 (d, J = 7.83 Hz, 1H), 8.63 (s, 2H), 9.03 (s, 1H), 11.09 (s, 1H); ^{13}C NMR (DMSO-d_6, 600 MHz) δ: 14.9, 31.3, 35.4, 42.9, 45.7, 64.1, 68.4, 71.1, 109.2, 115.6, 117.5, 127.9, 127.9, 129.2, 130.2, 130.9, 131.6, 131.7, 136.9, 137.8, 155.8, 155.9, 157.1, 157.5, 160.2, 161.8, 162.1. HRMS m/z calcd for $C_{37}H_{39}Cl_2N_7O_4$ [M - H]$^-$ 714.2368, found 714.2356. HPLC purity 98.5%. Retention time: 19.8 min, eluted with 10% n-hexane/90% isopropanol.

2-((1-(2-(4-(*Tert*-butyl)-2-ethoxyphenyl)-4,5-bis(4-chlorophenyl)-4,5-dihydro-1*H*-imidazole-1-carbonyl)piperidin-4-yl)amino)-*N*-hydroxypyrimidine-5-carboxamide (16a). The product was obtained as a white solid (0.27 g, 0.37 mmol), yield: 91.0%. ^{1}H NMR (DMSO-d_6, 600 MHz) δ: 0.81-0.95 (m, 2H), 1.33 (t, J = 7.17 Hz, 3H), 1.34 (s, 9H), 1.56 (d, J = 10.12 Hz, 1H), 1.58 (d, J = 10.12 Hz, 1H), 2.47 (t, J = 11.80 Hz, 2H), 2.59 (t, J = 11.38 Hz, 1H), 3.54-3.67 (m, 3H), 4.11 (dd, J = 13.91 Hz,

7.17 Hz, 2H), 5.55 (d, *J* = 10.12 Hz, 1H), 5.67 (d, *J* = 10.12 Hz, 1H), 6.97(d, *J* = 8.01 Hz, 2H), 7.01-7.08 (m, 4H), 7.12 (d, *J* = 8.43 Hz, 2H), 7.15 (d, *J* = 8.43 Hz, 2H), 7.51 (d, *J* = 8.01 Hz, 1H), 8.56 (s, 2H), 8.95 (s, 1H), 10.98 (s, 1H); ^{13}C NMR (DMSO-d_6, 600 MHz) δ: 14.9, 30.6, 30.9, 31.5, 35.4, 44.2, 44.7, 47.7, 64.0, 68.3, 71.7, 109.2, 115.3, 117.5, 118.1, 127.9, 129.2, 130.2, 130.6, 131.6, 137.1, 138.0, 155.2, 155.8, 156.7, 160.8, 162.5. HRMS m/z calcd for $C_{38}H_{41}Cl_2N_7O_4$ $[M + H]^+$ 730.2670, found 730.2679. HPLC purity 97.4%. Retention time: 19.3 min, eluted with 9% n-hexane/91% isopropanol.

(*E*)-1-(2-(4-(*tert*-butyl)-2-ethoxyphenyl)-4,5-bis(4-chlorophenyl)-4,5-dihydro-1 *H*-imidazole-1-carbonyl)-*N*-(4-(3-(hydroxyamino)-3-oxoprop-1-en-1-yl)phenyl)pi peridine-4-carboxamide (16b). The product was obtained as a white solid (0.36 g, 0.46 mmol), yield: 88.2%. ^{1}H NMR (DMSO-d_6, 600 MHz) δ: 1.21-1.25 (m, 2H), 1.34 (d, *J* = 6.85 Hz, 3H) 1.34 (s, 9H), 1.51 (d, *J* = 10.06 Hz, 2H), 2.23 (t, *J* = 11.39 Hz, 1H), 2.42 (t, *J* = 11.82 Hz, 1H) 2.54 (t, *J* = 12.85 Hz, 1H), 3.62 (d, *J* = 12.70 Hz, 1H), 3.67 (d, *J* = 12.70 Hz, 1H), 4.05-4.15 (m, 2H), 5.54 (d, *J* = 10.07 Hz, 1H), 5.68 (d, *J* = 10.07 Hz, 1H), 6.34 (d, *J* = 15.77 Hz, 1H), 6.98 (d, *J* = 7.88 Hz, 2H), 7.05 (t, *J* = 8.98 Hz, 3H), 7.08 (d, *J* = 8.76 Hz, 1H), 7.11 (d, *J* = 8.32 Hz, 2H), 7.17 (d, *J* = 8.32 Hz, 2H), 7.38 (d, *J* = 7.85 Hz, 1H),, 7.46 (d, *J* = 7.88 Hz, 2H), 7.52 (d, *J* = 7.88 Hz, 1H), 7.57 (d, *J* = 8.21 Hz, 2H), 8.97 (s, 1H), 9.89 (s, 1H), 10.69 (s, 1H); ^{13}C NMR (DMSO-d_6, 300 MHz) δ: 14.9, 27.6, 27.9, 30.1, 31.2, 31.4, 35.4, 42.3, 45.6, 64.0, 68.4, 71.1, 109.1, 117.5, 117.7, 119.5, 127.9, 128.5, 129.2, 129.9, 130.2, 130.6, 131.5, 131.6, 137.1, 138.0, 138.4, 140.9, 155.7, 155.8, 156.8, 160.5, 163.5, 173.1. HRMS

m/z calcd for $C_{43}H_{45}Cl_2N_5O_5$ $[M + H]^+$ 782.2817, found 782.2832. HPLC purity 95.1%. Retention time: 18.3 min, eluted with 5% n-hexane/95% isopropanol.

1-(2-(4-(*Tert*-butyl)-2-ethoxyphenyl)-4,5-bis(4-chlorophenyl)-4,5-dihydro-1*H*-imidazole-1-carbonyl)-*N*-hydroxypiperidine-4-carboxamide (17). The product was obtained as a white solid (0.25 g, 0.39 mmol), yield: 89.6%. ^{1}H NMR (DMSO-d_6, 600 MHz) δ: 0.81-0.87 (m, 2H), 1.23-1.40 (m, 5H), 1.35 (s, 9H), 1.86-1.90 (m, 1H), 2.23-2.48 (m, 2H), 3.58 (d, J = 8.18 Hz, 1H), 3.65 (d, J = 8.18 Hz, 1H), 4.10 (s, 2H), 5.59 (d, J = 8.98 Hz, 1H), 5.72 (d, J = 8.98 Hz, 1H), 6.94-7.18 (m, 10H), 7.52 (s, 1H), 8.58 (s, 1H), 10.26 (s, 1H); ^{13}C NMR (DMSO-d_6, 600 MHz) δ: 16.3, 29.1, 29.3, 32.8, 36.8, 40.2, 46.8, 65.4, 69.8, 71.9, 110.6, 118.9, 129.3, 129.3, 130.6, 131.5, 131.9, 133.1, 138.0, 139.1, 156.4, 157.6, 158.2, 162.5, 172.3. HRMS m/z calcd for $C_{34}H_{38}Cl_2N_4O_4$ $[M + H]^+$ 637.2343, found 637.2371. HPLC purity 96.3%. Retention time: 16.7 min, eluted with 5% n-hexane/95% isopropanol.

***In vitro* HDACs Inhibition Assay.** The HDAC1 enzyme was purchase from Abcam (#AB101661). All of the enzymatic reactions were conducted at 37 ^{o}C for 30 minutes. The reaction mixture contained 25 mM Tris (pH = 8.0), 1 mM $MgCl_2$, 0.1 mg/mL BSA, 137 mM NaCl, 2.7 mM KCl, HDAC1 and the enzyme substrate in a final volume of 50 μL. The compounds were diluted in 10% DMSO and 5 μL of the dilution was added to a 50 μL reaction so that the final concentration of DMSO was 1% in all of reactions. The assay was performed by quantitating the fluorescent product amount of in solution following an enzyme reaction. Fluorescence was then analyzed with an excitation of 350-360 nm and an emission wavelength of 450-460 nm at

Spectra Max M5 microtiter plate reader. The IC_{50} values were calculated using nonlinear regression with normalized dose-response fit using Prism GraphPad sofeware.

***In vitro* Antiproliferative Assay.** Cells were plated in 96-well transparent plates at a density of ~ 6×10^3/well and incubated in a humidified atmosphere with 5% CO_2 at 37 °C for 24 h. Test compounds were added onto triplicate wells with different concentrations and 0.1% DMSO for control. After they had been incubated for 72 h, 10 μL of cell counting kit-8 (CCK8) solution was added to each well and the plate was incubated for additional 0.5 h - 1 h. The absorbance (OD) was read on a Biotek Synergy H2 (Lab systems) at 405 nm. The concentration causing 50% inhibition of cell growth (IC_{50}) was determined by the Logit method. All experiments were performed three times.

Western Blotting. A549 cell lines were seeded (3.5×10^5 cells/well) on 6-well transparent plates (Corning). The inhibitors were added 24 h following seeding, and cells were incubated for additional 24 h, then, washed with cold-ice PBS for 2 times and 60 μL ice-cold lysis buffer containing 1% protease and phosphatase inhibitors (Roche). Cells were scraped off after 30 min on ice and centrifuged for 12,000 rpm for 15 min at 4 °C to obtain the protein lysate. The protein extract was denatured at 100 °C bath and analyzed on 10%-15% SDS-PAGE gels. The gels were blotted onto PVDF membrane (Merck Millipore) and blocked with 5% BSA Buffer (5% Albumin Bovine V from Bovine serum in TBST) for 2 h at room temperature. The primary antibodies used for Western boltting were: p53 (Abcam, ab7757), MDM2 (Abcam,

ab16895), Histone 3 (Abcam, ab47915), Histone 4 (Abcam, ab177790), Acetyl-α-tublin (Abcam, ab24610), GAPDH (Abcam, ab181602). Then, the membranes were infrared secondary antibodies. After washing with TBST for 3 times, blots were scanned on a LI-COR Odyssey imaging system. The protein levels were quantified by the gray values of the bands in the resulting images using the control group as the standard.

Cell Cycle Analysis by Flow Cytometry. A549 cells (3.5×10^5 cells/well) were treated with compounds at 1 μM and 10 μM for 48 h. The treated cells were collected, resuspended, and then, incubated for 30 min at 37 °C with 300 μL DNA staining solution and 5 μL permeabilization solution (Cell Cycle Staining Kit, MultiSciences, 70-CCS012). For each sample, at least 1×10^4 cells were analyzed using flow cytometry (BD Accuri C6).

Apoptosis Detection Assay. A549 cells (3.5×10^5 cells/well) were seeded in six-well plates and treated with compounds at concentration of 10 μM and 20 μM for 48 h. the cells were then harvested by trypsinization and washed twice with cold PBS. After centrifugation and removal of the supernatants, cells were resuspended in 400 μL of 1 × binding buffer which was then added to 5 μL of annexin V-FITC and incubated at room temperature for 15 min. After adding 10 μL of PI the cells were incubated at room temperature for another 15 min in dark. The stained cells were analyzed by a Flow Cytometer (BD Accuri C6).

***In vivo* Antitumor Potency.** The experimental procedures and the animal use and care protocols were approved by the Committee on Ethical Use of Animals of Second

Military Medical University. BALB/C nude female mice (certificate SCXK-2007-0005, weighing 18−20 g) were obtained from Shanghai Experimental Animal Center, Chinese Academy of Sciences. For *in vivo* efficacy experiments using the A549 tumor xenograft model, A549 cells (5×10^6 cells/animal) were injected subcutaneously into the flank area of the female nude mice (6-7 weeks old). When tumors reached about a volume of 100 mm^3, mice were randomized into five groups of treatment and control groups (5 mice per treatment group and 7 mice for the vehicle control group). The four treatment groups received compound **14d** (100 mg/kg/day or 150 mg/kg/day), **1** (100 mg/kg/day) or **3** (100 mg/kg/day) by oral administration once per day for 21 days, and the vehicle control group received equal volume of normal saline solution. During treatment, tumor growth was measured with a vernier caliper about every three days, and body weight was monitored at the same time. The tumor volume was evaluated by the length and width of the tumor tissues. Tumor volume was calculated according to the formula, volume = $(AB^2)/2$, where A and B are the tumor length and width dimension, respectively. Data were analyzed by two-tailed t test. P level < 0.05 was considered statistically significant.

■ ASSOCIATED CONTENT

Supporting Information

The Supporting Information is available free of charge on the ACS Publications website at DOI: XXXXXX/acs.jmedchem.XXXXXXX.

Authors will release the atomic coordinates upon article publication.

The solubility of representative compounds, the chiral separation of racemic **14d**, the identification of configuration of enantiomers **14d**, chemical synthesis and structural characterization of intermediates, solubility assay, methods for pharmacokinetic studies and molecular docking, ^{1}H NMR and ^{13}C NMR spectra of the representative compounds.

SMILES molecular formula strings (CSV)

The binding mode of compound 14d enantiomers with MDM2 and HDAC1 (PDB)

■ AUTHOR INFORMATION

Corresponding Author

* (C. S.) Phone / Fax: +86 21 81871239. E-mail: shengcq@smmu.edu.cn

* (W. W.) E-mail: wwang@unm.edu

* (Z. M.) Phone / Fax: +86 21 81871241. E-mail: miaozhenyuan@hotmail.com

Author Contributions

† S. H., G. D. and S. W. contributed equally to this work.

The manuscript was written through contributions of all authors. All authors have given approval to the final version of the manuscript.

Notes

The authors declare no competing financial interest.

■ ACKNOWLEDGMENT

This work was supported by the National Natural Science Foundation of China (Grants 21738002 to W. W., 81673352 to Z. M. and 81725020 to C. S.), and the National Key R&D Program of China (2017YFA0506000 to C. S.).

■ ABBREVIATIONS LIST

HDAC, histone deacetylase; MDM2, murine double-minute 2; SD, Sprague-Dawley; SEM, Standard Error of Mean; BTC, Bis-(trichloromethyl)-carbonate; DIPEA, *N,N*-Diisopropylethylamine; DMF, dimethylformamide; HBTU, O-Benzotriazole-N,N,N',N'-tetramethyl-uronium-hexafluorophosphate; PI, propidium iodide; ZBG, zinc-binding group; TGI, tumor growth inhibition

REFERENCES

1. Lane, D. P. Cancer. p53, guardian of the genome. *Nature* **1992**, *358*, 15-16.

2. Vogelstein, B.; Lane, D.; Levine, A. J. Surfing the p53 network. *Nature* **2000**, *408*, 307-310.

3. Hainaut, P.; Hollstein, M. P53 and human cancer: the first ten thousand mutations. *Adv. Cancer Res.* **2000**, *77*, 81-137.

4. Vousden, K. H.; Lane, D. P. P53 in health and disease. *Nat. Res. Mol. Cell Biol.* **2007**, *8*, 275-283.

5. Momand, J.; Wu, H. H.; Dasgupta, G. MDM2-master regulator of the p53 tumor suppressor protein. *Gene* **2000**, *242*, 15-29.

6. Bond, G. L.; Hu, W.; Levine, A. J. MDM2 is a central node in the p53 pathway: 12 years and counting. *Curr. Cancer Drug Targets* **2005**, *5*, 3-8.

7. Hu, W.; Feng, Z.; Levine, A. J. The regulation of multiple p53 stress responses is mediated through MDM2. *Genes Cancer* **2012**, *3*, 199-208.

8. Wade, M.; Wang, Y. V.; Wahl, G. M. The p53 orchestra: Mdm2 and mdmx set

the tone. *Trends Cell Biol.* **2010**, *20*, 299-309.

9. Wang, S.; Zhao, Y.; Bernard, D.; Aguilar, A.; Kumar, S. Targeting the MDM2-p53 protein-protein interaction for new cancer therapeutics. *Cold Spring Barbor Perspect. Med.* **2012**, 57-79.

10. Estrada-Ortiz, N.; Neochoritis, C. G.; Domling, A. How to design a successful p53-MDM2/X interaction inhibitor: a thorough overview based on crystal structures. *ChemMedChem* **2016**, *11*, 757-772.

11. Estrada-Ortiz, N.; Neochoritis, C. G.; Twarda-Clapa, A.; Musielak, B.; Holak, T. A.; Domling, A. Artificial macrocycles as potent p53-MDM2 inhibitors. *Acs Med. Chem. Lett.* **2017**, *8*, 1025-1030.

12. Surmiak, E.; Neochoritis, C. G.; Musielak, B.; Twarda-Clapa, A.; Kurpiewska, K.; Dubin, G.; Camacho, C.; Holak, T. A.; Domling, A. Rational design and synthesis of 1,5-disubstituted tetrazoles as potent inhibitors of the MDM2-p53 interaction. *Eur. J. Med. Chem.* **2017**, *126*, 384-407.

13. Zhao, Y.; Aguilar, A.; Bernard, D.; Wang, S. Small-molecule inhibitors of the MDM2-p53 protein-protein interaction (MDM2 inhibitors) in clinical trials for cancer treatment. *J. Med. Chem.* **2015**, *58*, 1038-1052.

14. Popowicz, G. M.; Doemling, A.; Holak, T. A. The structure-based design of mdm2/mdmx-p53 inhibitors gets serious. *Angew. Chem., Int. Ed.* **2011**, *50*, 2680-2688.

15. Iancu-Rubin, C.; Mosoyan, G.; Glenn, K.; Gordon, R. E.; Nichols, G. L.; Hoffman, R. Activation of p53 by the MDM2 inhibitor RG7112 impairs

thrombopoiesis. *Exp. Hematol.* **2014**, *42*, 137-145.

16. Wagner, A. J.; Banerji, U.; Mahipal, A.; Somaiah, N.; Hirsch, H. A.; Fancourt, C.; Levonas, A.; Lam, R.; Meister, A.; Kemp, R. K.; Knox, C.; Rose, S.; Hong, D. S. A phase I trial of the human double minute 2 (HDM2) inhibitor MK-8242 in patients (pts) with advanced solid tumors. *J. Clin. Oncol.* **2015**, *33*, 1304-1311.

17. Siu, L. L.; Italiano, A.; Miller, W. H.; Blay, J.-Y.; Gietema, J. A.; Bang, Y.-J.; Mileshkin, L. R.; Hirte, H. W.; Reckner, M.; Higgins, B.; Jukofsky, L.; Blotner, S.; Zhi, J.; Middleton, S.; Nichols, G. L.; Chen, L. C. Phase 1 dose escalation, food effect, and biomarker study of RG7388, a more potent second-generation MDM2 antagonist, in patients (pts) with solid tumors. *J. Clin. Oncol.* **2014**, *32*, (Suppl.) 2535.

18. Singh, A. K.; Chauhan, S. S.; Singh, S. K.; Verma, V. V.; Singh, A.; Arya, R. K.; Maheshwari, S.; Akhtar, M. S.; Sarkar, J.; Rangnekar, V. M.; Chauhan, P. M. S.; Datta, D. Dual targeting of MDM2 with a novel small-molecule inhibitor overcomes TRAIL resistance in cancer. *Carcinogenesis* **2016**, *37*, 1027-1040.

19. de Lera, A. R.; Ganesan, A. Epigenetic polypharmacology: from combination therapy to multitargeted drugs. *Clin Epigenet.* **2016**, *8*, 1-21.

20. Zhuang, C.; Miao, Z.; Wu, Y.; Guo, Z.; Li, J.; Yao, J.; Xing, C.; Sheng, C.; Zhang, W. Double-edged swords as cancer therapeutics: novel, orally active, small molecules simultaneously inhibit p53-MDM2 interaction and the NF-kappa B pathway. *J. Med. Chem.* **2014**, *57*, 567-577.

21. Zhuang, C.; Miao, Z.; Zhu, L.; Dong, G.; Guo, Z.; Wang, S.; Zhang, Y.; Wu, Y.; Yao, J.; Sheng, C.; Zhang, W. Discovery, synthesis, and biological evaluation of

orally active pyrrolidone derivatives as novel inhibitors of p53-MDM2 protein-protein interaction. *J. Med. Chem.* **2012**, *55*, 9630-9642.

22. Kouzarides, T. Chromatin modifications and their function. *Cell* **2007**, *128*, 693-705.

23. Ropero, S.; Esteller, M. The role of histone deacetylases (HDACs) in human cancer. *Mol. Oncol.* **2007**, *1*, 19-25.

24. Mann, B. S.; Johnson, J. R.; Cohen, M. H.; Justice, R.; Pazdur, R. FDA approval summary: vorinostat for treatment of advanced primary cutaneous T-cell lymphoma. *Oncologist* **2007**, *12*, 1247-1252.

25. Grant, C.; Rahman, F.; Piekarz, R.; Peer, C.; Frye, R.; Robey, R. W.; Gardner, E. R.; Figg, W. D.; Batest, S. E. Romidepsin: a new therapy for cutaneous T-cell lymphoma and a potential therapy for solid tumors. *Expert Rev. Anticancer Ther.* **2010**, *10*, 997-1008.

26. Tan, J.; Cang, S.; Ma, Y.; Petrillo, R. L.; Liu, D. Novel histone deacetylase inhibitors in clinical trials as anti-cancer agents. *J. Hematol. Oncol.* **2010**, *3*, 5.

27. Federico, M.; Bagella, L. Histone deacetylase inhibitors in the treatment of hematological malignancies and solid tumors. *J. Biomed. Biotechnol.* **2011**, *2011*, 475641-475641.

28. Ong, P. S.; Wang, X. Q.; Lin, H. S.; Chan, S. Y.; Ho, P. C. Synergistic effects of suberoylanilide hydroxamic acid combined with cispiatin causing cell cycle arrest independent apoptosis in platinum-resistant ovarian cancer cells. *Int. J. Oncol.* **2012**, *40*, 1705-1713.

29. Kim, J. C.; Shin, E. S.; Kim, C. W.; Roh, S. A.; Cho, D. H.; Na, Y. S.; Kim, T. W.; Kim, M. B.; Hyun, Y. L.; Ro, S.; Kim, S. Y.; Kim, Y. S. In vitro evaluation of histone deacetylase inhibitors as combination agents for colorectal cancer. *Anticancer Res.* **2009**, *29*, 3027-3034.

30. De Schutter, H.; Nuyts, S. Radiosensitizing potential of epigenetic anticancer drugs. *Anti-Cancer Agents Med. Chem.* **2009**, *9*, 99-108.

31. Zhu, W. G.; Otterson, G. A. The interaction of histone deacetylase inhibitors and DNA methyltransferase inhibitors in the treatment of human cancer cells. *Curr. Med. Chem.: Anti-cancer Agents* **2003**, *3*, 187-199.

32. Morphy, R.; Kay, C.; Rankovic, Z. From magic bullets to designed multiple ligands. *Drug Discovery Today* **2004**, *9*, 641-651.

33. Anighoro, A.; Bajorath, J.; Rastelli, G. Polypharmacology: challenges and opportunities in drug discovery. *J. Med. Chem.* **2014**, *57*, 7874-7887.

34. He, S.; Dong, G.; Wang, Z.; Chen, W.; Huang, Y.; Li, Z.; Jiang, Y.; Liu, N.; Yao, J.; Miao, Z.; Zhang, W.; Sheng, C. Discovery of novel multiacting topoisomerase I/II and histone deacetylase inhibitors. *Acs Med. Chem. Lett.* **2015**, *6*, 239-243.

35. Dong, G.; Chen, W.; Wang, X.; Yang, X.; Xu, T.; Wang, P.; Zhang, W.; Rao, Y.; Miao, C.; Sheng, C. Small molecule inhibitors simultaneously targeting cancer metabolism and epigenetics: discovery of novel nicotinamide phosphoribosyltransferase (NAMPT) and histone deacetylase (HDAC) dual inhibitors. *J. Med. Chem.* **2017**, *60*, 7965-7983.

36. Ganesan, A. Multitarget drugs: an epigenetic epiphany. *Chemmedchem* **2016**, *11*,

1227-1241.

37. Bolden, J. E.; Peart, M. J.; Johnstone, R. W. Anticancer activities of histone deacetylase inhibitors. *Nat. Rev. Drug Discovery* **2006**, *5*, 769-784.

38. Tesei, A.; Brigliadori, G.; Carloni, S.; Fabbri, F.; Ulivi, P.; Arienti, C.; Sparatore, A.; Del Soldato, P.; Pasini, A.; Amadori, D.; Silvestrini, R.; Zoli, W. Organosulfur derivatives of the HDAC inhibitor valproic acid sensitize human lung cancer cell lines to apoptosis and to cisplatin cytotoxicity. *J. Cell. Physiol.* **2012**, *227*, 3389-3396.

39. Hubbert, C.; Guardiola, A.; Shao, R.; Kawaguchi, Y.; Ito, A.; Nixon, A.; Yoshida, M.; Wang, X. F.; Yao, T. P. HDAC6 is a microtubule-associated deacetylase. *Nature* **2002**, *417*, 455-458.

40. McCormack, E.; Haaland, I.; Venas, G.; Forthun, R. B.; Huseby, S.; Gausdal, G.; Knappskog, S.; Micklem, D. R.; Lorens, J. B.; Bruserud, O.; Gjertsen, B. T. Synergistic induction of p53 mediated apoptosis by valproic acid and nutlin-3 in acute myeloid leukemia. *Leukemia* **2012**, *26*, 910-917.

41. Oliner, J. D.; Pietenpol, J. A.; Thiagalingam, S.; Gyuris, J.; Kinzler, K. W.; Vogelstein, B. Oncoprotein MDM2 conceals the activation domain of tumour suppressor p53. *Nature* **1993**, *362*, 857-860.

42. Wu, X.; Bayle, J. H.; Olson, D.; Levine, A. J. The p53-mdm2 autoregulatory feedback loop. *Genes Dev.* **1993**, *7*, 1126-1132.

43. Kubbutat, M. H.; Jones, S. N.; Vousden, K. H. Regulation of p53 stability by mdm2. *Nature* **1997**, *387*, 299-303.

44. Tweddle, D. A.; Malcolm, A. J.; Bown, N.; Pearson, A. D.; Lunec, J. Evidence

for the development of p53 mutations after cytotoxic therapy in a neuroblastoma cell line. *Cancer Res.* **2001**, *61*, 8-13.

45. Condorelli, F.; Gnemmi, I.; Vallario, A.; Genazzani, A. A.; Canonico, P. L. Inhibitors of histone deacetylase (HDAC) restore the p53 pathway in neuroblastoma cells. *Br. J. Pharmacol.* **2008**, *153*, 657-668.

46. Xu, W. S.; Parmigiani, R. B.; Marks, P. A. Histone deacetylase inhibitors: molecular mechanisms of action. *Oncogene* **2007**, *26*, 5541-5552.

47. Vassilev, L. T.; Vu, B. T.; Graves, B.; Carvajal, D.; Podlaski, F.; Filipovic, Z.; Kong, N.; Kammlott, U.; Lukacs, C.; Klein, C.; Fotouhi, N.; Liu, E. A. In vivo activation of the p53 pathway by small-molecule antagonists of MDM2. *Science* **2004**, *303*, 844-848.

48. Secchiero, P.; Bosco, R.; Celeghini, C.; Zauli, G. Recent advances in the therapeutic perspectives of nutlin-3. *Curr. Pharm. Des.* **2011**, *17*, 569-577.

49. Vu, B.; Wovkulich, P.; Pizzolato, G.; Lovey, A.; Ding, Q.; Jiang, N.; Liu, J.-J.; Zhao, C.; Glenn, K.; Wen, Y.; Tovar, C.; Packman, K.; Vassilev, L.; Graves, B. Discovery of RG7112: a small-molecule MDM2 inhibitor in clinical development. *Acs Med. Chem. Lett.* **2013**, *4*, 466-469.

50. Miller, T. A.; Witter, D. J.; Belvedere, S. Histone deacetylase inhibitors. *J. Med. Chem.* **2003**, *46*, 5097-5116.

51. Wang, D. F.; Wiest, O.; Helquist, P.; Lan-Hargest, H. Y.; Wiech, N. L. On the function of the 14 A long internal cavity of histone deacetylase-like protein: implications for the design of histone deacetylase inhibitors. *J. Med. Chem.* **2004**, *47*,

3409-3417.

52. Allen, J. G.; Bourbeau, M. P.; Wohlhieter, G. E.; Bartberger, M. D.; Michelsen, K.; Hungate, R.; Gadwood, R. C.; Gaston, R. D.; Evans, B.; Mann, L. W.; Matison, M. E.; Schneider, S.; Huang, X.; Yu, D.; Andrews, P. S.; Reichelt, A.; Long, A. M.; Yakowec, P.; Yang, E. Y.; Lee, T. A.; Oliner, J. D. Discovery and optimization of chromenotriazolopyrimidines as potent inhibitors of the mouse double minute 2-tumor protein 53 protein-protein interaction. *J. Med. Chem.* **2009**, *52*, 7044-7053.

53. Mai, A.; Massa, S.; Rotili, D.; Cerbara, I.; Valente, S.; Pezzi, R.; Simeoni, S.; Ragno, R. Histone deacetylation in epigenetics: an attractive target for anticancer therapy. *Med. Res. Rev.* **2005**, *25*, 261-309.

54. Kussie, P. H.; Gorina, S.; Marechal, V.; Elenbaas, B.; Moreau, J.; Levine, A. J.; Pavletich, N. P. Structure of the MDM2 oncoprotein bound to the p53 tumor suppressor transactivation domain. *Science* **1996**, *274*, 948-953.

55. Ding, K.; Lu, Y.; Nikolovska-Coleska, Z.; Wang, G.; Qiu, S.; Shangary, S.; Gao, W.; Qin, D.; Stuckey, J.; Krajewski, K.; Roller, P. P.; Wang, S. Structure-based design of spiro-oxindoles as potent, specific small-molecule inhibitors of the MDM2-p53 interaction. *J. Med. Chem.* **2006**, *49*, 3432-3435.

56. Shu, L.; Wang, P.; Liu, W.; Gu, C. A practical synthesis of a cis-4,5-bis(4-chlorophenyl)imidazoline intermediate for nutlin analogues. *Org. Process Res. Dev.* **2012**, *16*, 1866-1869.

57. Patil, V.; Sodji, Q. H.; Kornacki, J. R.; Mrksich, M.; Oyelere, A. K. 3-Hydroxypyridin-2-thione as novel zinc binding group for selective histone

deacetylase inhibition. *J. Med. Chem.* **2013**, *56*, 3492-3506.

58. Nome, R. V.; Bratland, A.; Harman, G.; Fodstad, O.; Andersson, Y.; Ree, A. H. Cell cycle checkpoint signaling involved in histone deacetylase inhibition and radiation-induced cell death. *Mol. Cancer Ther.* **2005**, *4*, 1231-1238.

59. Wong, C. F.; Guminski, A.; Saunders, N. A.; Burgess, A. J. Exploiting novel cell cycle targets in the development of anticancer agents. *Curr. Cancer Drug Targets* **2005**, *5*, 85-102.

60. Henderson, C.; Mizzau, M.; Paroni, G.; Maestro, R.; Schneider, C.; Brancolini, C. Role of caspases, Bid, and p53 in the apoptotic response triggered by histone deacetylase inhibitors trichostatin-A (TSA) and suberoylanilide hydroxamic acid (SAHA). *J. Biol. Chem.* **2003**, *278*, 12579-12589.

61. Pont, L. M. E. B.; Naipal, K.; Kloezeman, J. J.; Venkatesan, S.; van den Bent, M.; van Gent, D. C.; Dirven, C. M. F.; Kanaar, R.; Lamfers, M. L. M.; Leenstra, S. DNA damage response and anti-apoptotic proteins predict radiosensitization efficacy of HDAC inhibitors SAHA and LBH589 in patient-derived glioblastoma cells. *Cancer Lett.* **2015**, *356*, 525-535.

62. Proskurnina, M. V.; Lozinskaya, N. A.; Tkachenko, S. E.; Zefirov, N. S. Reaction of aromatic aldehydes with ammonium acetate. *Russ. J. Org. Chem.* **2002**, *38*, 1149-1153.

Table of Contents Graphic

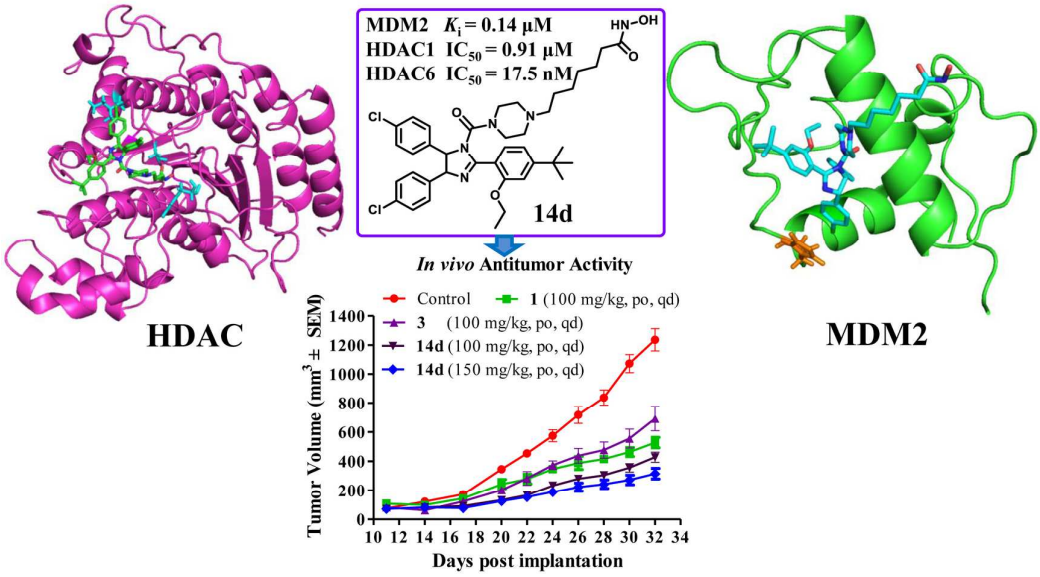

ACS Paragon Plus Environment